

TR/BR-16/98-99

DEVELOPMENT OF A DISTRIBUTED CATCHMENT MODEL



**NATIONAL INSTITUTE OF HYDROLOGY
JALVIGYAN BHAWAN
ROORKEE - 247 667 (UTTARANCHAL)**


1998-99

PREFACE

Modeling of rainfall-runoff process is important for water resources management, safe yield computations and design of flood control structures. The runoff production is complicated by various distributed hydrologic components. The rainfall-runoff models should represent the physical controls of soil, vegetation and topography on runoff production. Lumped models ignore spatially distributed watershed properties and consider only the spatially averaged inputs. The influence of geomorphologic and climatic factors is represented in distributed models. Distributed models require large amount of data compared to lumped models. Geographic Information System (GIS) is an effective and convenient tool for the hydrological modeling to study the basin characteristics and their influence on runoff generation.

In this study, a spatially distributed unit hydrograph was developed using GIS ARC/INFO for the Kolar basin in the Madhya Pradesh State. The SCS CN method was used to derive the effective rainfall hyetograph. The grid module of GIS ARC/INFO was used to develop the Digital Elevation Model, slope map and equivalent drainage network required in the construction of isochrone map. The spatially distributed unit hydrograph was derived using the time-area (S hydrograph) diagram developed from the isochrone map. The hydrograph computed from the spatially distributed unit hydrograph using the storm events were evaluated with the observed hydrographs. Better match was observed in few storm events.

This report has been prepared by Sh A. R. Senthil kumar, Scientist 'B' (Water Resources Systems Div.), Sh. M. K. Jain, Scientist 'C' (Watershed Development Division), Dr. S. K. Jain, Scientist 'F' (Water Resources Systems Div.) and Sh. P. K. Agarwal, SRA (Water Resources Systems Div.) of this Institute.


(K S Ramasastri)
Director

ABSTRACT

The rainfall-runoff relationships are the most complex hydrologic phenomena to model due to large amount of spatial and temporal variability of watershed characteristics. Distributed models have been developed to represent the variability in physical watershed characteristics.

In this study a spatially distributed unit hydrograph was developed using ARC/INFO GIS package. The catchment of Kolar basin up to Satrana (863.125 sq.km.) in Madhya Pradesh was selected for this study. The rainfall values for Brijeshnagar, Birpur and Jholiapur rainfall stations and the runoff values for the Satrana gauging site were used for developing the model. Landuse details were derived from FCC of IRS LISS II of path/row 27/52 and 28/51 of post monsoon season, 1989. SCS CN method has been used to derive the effective rainfall hyetograph. The GRID module of GIS ARC/INFO was used to develop and compile isochrone map by summing up the time of concentration in each grid cell. S hydrograph technique has been used to derive the spatially distributed unit hydrograph. Six storms (19.08.1983, 09.08.1984, 30.07.1985, 13.08.1985, 14.08.1986 and 26.08.1987) were considered for the comparison of the convoluted direct runoff hydrographs with the observed hydrographs. The time to peak and peak discharge of event number 3 and 6 are matching better than other storm events.

CONTENTS

	Page no.
LIST OF TABLES AND FIGURES	ii
1.0 INTRODUCTION	1
1.1 Purpose and Scope of this Report	2
2.0 REVIEW OF LITERATURE	3
3.0 METHODOLOGY	6
3.1 Determination of Effective Rainfall	6
3.2 The Eight Directional Cell Flow Model	11
3.3 Flow routing in the cell	11
3.4 Calculation of travel time	11
3.4.1 Overland flow travel time	12
3.4.2 Travel times in the channel	12
3.5 Time-Area diagram	13
3.6 Distributed Unit Hydrograph	14
3.7 Direct Runoff Hydrograph	15
4.0 THE STUDY AREA	17
4.1 The Kolar Basin	17
4.2 Data Availability	18
5.0 DEVELOPMENT OF THE DISTRIBUTED MODEL	19
5.1 The GIS ARC/INFO	19
5.2 Generation of Input Grid Maps	19
5.3 Calculation of Effective Rainfall	20
5.4 Derivation of Time-Area diagram	21
5.5 Determination of Direct Runoff Hydrograph	22
6.0 DISCUSSION OF RESULTS	23
7.0 CONCLUSIONS	26
REFERENCES	28
TABLES AND FIGURES	30

LIST OF TABLES AND FIGURES

		Page no.
Table 1	Seasonal Rainfall Limits for Three Level of Antecedent Moisture Condition (AMC)	30
Table 2(a)	Runoff Curve Number for Urban areas	30
Table 2(b)	Runoff Curve Numbers for Cultivated Agricultural lands	31
Table 2(c)	Runoff Curve Numbers for Other Cultivated Agricultural lands	32
Table 2(d)	Runoff curve Numbers for Arid and Semiarid Rangelands	33
Table 3	Spectral signature of different landuse categories	34
Table 4	Spatially averaged rainfall data for the events considered for the simulation	35
Table 5	The observed discharge data (minus base flow) at Satrana for the events considered for the simulation	36
Table 6	Curve numbers for different landuse and soil type for AMC II	37
Table 7	Adjusted initial abstraction parameter for the different storm events considered for the simulation	37
Table 8	Rainfall excess using SCS CN method for the storm events considered for the simulation	38
Table 9	Manning's n for different landuses	39
Table 10	Incremental isochronal area for 1 hour interval of time of concentration	39
Table 11	The simulated direct runoff values for the events considered	40
Table 12	Peak flow and time to peak flow of observed and simulated direct runoff for the events considered	41
Figure 1	Watershed Terrain Analysis using Grid GIS Methods	42
Figure 2	Flow routing in the cell	42
Figure 3	Watershed Time-Area Relationships	43
Figure 4	Time-Area Diagram and the Unit Hydrograph	44
Figure 5	Index Map of Kolar Basin up to Satrana gauging site	45
Figure 6	Drainage Map for Kolar Basin	46
Figure 7	Landuse Map for Kolar Basin	47

Figure 8	Soil group map for Kolar Basin	48
Figure 9	Thiessen Polygon Map for Kolar Basin	49
Figure 10	Digital Elevation Model (DEM) for Kolar Basin	50
Figure 11	Equivalent Drainage Network for Kolar Basin	51
Figure 12	Curve Number Map for Kolar Basin	52
Figure 13	Slope Map for Kolar Basin	53
Figure 14	Isochrone Map for Kolar basin	54
Figure 15	Time-Area Diagram for Kolar Basin	55
Figure 16	One hour Distributed Unit Hydrograph	55
Figure 17	Observed and Simulated Runoff for the Storm Event 1 (19.8.1983)	56
Figure 18	Observed and Simulated Runoff for the Storm Event 2 (9.8.1984)	57
Figure 19	Observed and Simulated Runoff for the Storm Event 3 (30.7.1985)	58
Figure 20	Observed and Simulated Runoff for the Storm Event 4 (13.8.1985)	59
Figure 21	Observed and Simulated Runoff for the Storm Event 5 (14.8.1986)	60
Figure 22	Observed and Simulated Runoff for the Storm Event 6 (26.8.1987)	61

CHAPTER 1

INTRODUCTION

Water is one of the most important natural resources of a country, which control the human development activities and it very much influences the living things. Planning and execution of water resources projects require stream flow data. Rainfall – runoff models have been developed to estimate the stream flow. The rainfall – runoff models should capture the essence of the physical controls of soil, vegetation, and topography on runoff production. A variety of rainfall – runoff models are available and those models are commonly classified as either lumped models or distributed parameter models.

The unit hydrograph is a lumped linear model that can be used to derive the surface runoff hydrograph resulting from any amount of excess rainfall. Sherman first proposed the unit hydrograph concept in 1932. The unit hydrograph of a watershed is defined as a direct runoff hydrograph resulting from unit depth of excess rainfall generated uniformly over the drainage area at a constant rate for an effective duration (Chow et al., 1988). Mathematical representation of the unit hydrograph has a long history in hydrology. Clark (1945) formulated a unit hydrograph model by combining the time – area diagram of the watershed with a linear reservoir at the outlet. Nash (1957) proposed a cascade of linear reservoirs as a unit hydrograph model and Dooge (1959) presented a unit hydrograph theory combining linear channels and linear reservoirs. The partial time - area diagram was proposed by Betson in 1964 in which the concept of source areas contributing to flow which expand and contract with time as the storm passes over watershed was considered. The theory of the geomorphic instantaneous unit hydrograph was proposed by Rodriguez-Iturbe & Valdes (1979) in which Horton's stream laws are used to integrate over the watershed the delay effect of channel links characterized by a mean holding time to produce a unit hydrograph as the probability density function of travel time of water to the outlet. This approach implicitly assumes that the runoff is produced by Hortonian overland flow throughout the watershed.

The unit hydrograph is a traditional means of representing the linear system response at the watershed outlet to rainfall over the watershed, but it suffers from the limitation that the response function is lumped over the whole watershed and does not explicitly account for the spatially distributed nature of watershed properties. To overcome this limitations, Geographic Information System (GIS) based new methodology has been proposed by Maidment (1993) and Muzik (1996). This new GIS based methodology allows the development of channel network for the calculation of realistic travel times, it handles the distributed excess rainfall in calculating local surface runoff rates as inputs for channel flow and it compiles the time – area diagram from which the distributed unit hydrograph is derived. With the GIS facility, it is possible to represent the land surface elevation over the watershed by a digital elevation model.

1.1 The Purpose and scope of this report

The aim of the report is to derive spatially distributed unit hydrograph for Kolar basin using the methodology as suggested by Muzik (1996). This spatially distributed unit hydrograph is used to derive the direct runoff hydrograph by convoluting the rainfall excess hyetograph of storm events. In this methodology SCS CN method is used to calculate the excess rainfall hyetograph.

CHAPTER 2

REVIEW OF LITERATURE

Hydrologic studies concerned with the design, river forecasting, land use, sedimentation, pollutant transport, etc., require to develop the relation between rainfall and runoff. The development of many rainfall-runoff models has been reported in literature since last century. The recent introduction of GIS into the field of rainfall – runoff modeling provides the facility to construct the distributed hydrological models to have better results than the other traditional modeling technique. Many distributed rainfall – runoff models with the use of GIS have been reported in journals. Some of them are briefly reviewed as follows.

Maidment (1993) developed a spatially distributed unit hydrograph using GIS. The spatially distributed unit hydrograph presented by him is similar to the concept of the geomorphic instantaneous unit hydrograph. GIS was used to describe the connectivity of the links in the watershed flow network. The routine based on the eight-direction flow model (pour point model) of the GIS package was used to derive the connectivity of the links in the watershed flow network with the use of digital elevation model. The velocity function $V = aS^b$ was used to define the velocity in each grid. The S in the equation is land surface slope and a and b are coefficients related to landuse. The watershed flow network derived by GIS and the velocity in each grid were used to compile the isochrones of the travel time of the watershed. The time-area diagram was derived from the compiled isochrones. The ordinates of the spatially distributed hydrograph were derived by the calculation of the slope of the time-area diagram over the specified time interval. The direct runoff hydrograph was derived by convoluting the spatially distributed unit hydrograph with excess rainfall hyetograph. The excess rainfall hyetograph was calculated by SCS CN method. This methodology was supported with an example of application.

Maidment et al (1996) proposed a model in which the watershed was decomposed into subareas consisting of individual cells or zones of neighbor cells. The unit

hydrograph was found to each subarea and the response at the outlet to excess rainfall on each subarea was summed to produce the watershed runoff hydrograph. The cell to cell flow path to the watershed outlet was determined from a digital elevation model. A constant flow velocity was assigned to each cell and the time lag between subarea input and the response at the watershed outlet was found by integrating the flow time along the path from the subarea to the outlet. The response function for a subarea was modelled as a lagged linear reservoir in which the flow time is equal to the sum of a time of translation and an average residence time in the reservoir. The developed model was applied to the Severn watershed at Plynlimon in Wales, UK. It was observed that the derived unit hydrograph by this model was closely matching with the flow records of the watershed. However, the observed peak discharge and the lag time were not matching with the developed hydrograph by this model.

Muzik (1996) presented a methodology to develop a spatially distributed unit hydrograph based on the fact that the unit hydrograph can be derived from the time-area curve of a watershed by the S-curve method. The method described by Maidment (1993) was used to derive the unit hydrograph from S-hydrograph. The capability of GIS was used to determine the accurate time-area diagram. The in-built routine of eight-direction flow model of GIS was used to derive the watershed channel network from the digital elevation model. SCS CN method was used to determine the average excess rainfall intensity based on the land use and soil type for Antecedent Moisture Condition II. The length of the derived watershed flow network was used to find the over land flow travel and the channel flow times. Overland flow travel times were calculated by the kinematic wave equation for time to equilibrium and the channel flow times were based on the Manning and continuity equations. The time to equilibrium is defined as the time equal to or greater than the time of concentration in which the flow results from an excess rainfall over the contributing area. Travel times were increased by a percentage depending on the channel reach and geometry to account for channel storage. The developed methodology was applied to Waiparous Creek in the Alberta foothills, Canada. The catchment area is 229 sq.km. The grid size of the study was 1000 m. The derived unit hydrograph gave excellent results in simulating the observed hydrograph. It was

observed that the distributed unit hydrograph could be a very promising new tool for the prediction of flood hydrographs.

Polarski (1997) presented a simple distributed rainfall – runoff model based on the discrete representation of variables. The types of hydrological processes modelled were throughflow (described by modified version of Darcy's law), channel flow (described by Manning's equation) and the interception-evaporation process as dependent on the presence or absence of forest canopy. The variables modeled were wetness, velocity and evaporation rate. Velocity was assigned in a fixed direction, the direction of steepest slope, but its magnitude vary spatially according to catchment properties, and also through time, as a function of local wetness. Evaporation was allowed to vary across space as a function of vegetation type. All variables were assumed constant within a time step and within a 50 m cell, except when a river runs through the cell, in which instance, the soil and channel are differentiated. The integration of processes over space yielded predictions of catchment evaporation and flow, as well as a prediction of the extent of the river network and variation in catchment wetness. Eight-direction cell flow model was used to derive the drainage network and the boundary of the catchment. This model was applied to a small catchment, the Upper Severn at Plynlimon Flume in the hills of mid Wales, U.K.

CHAPTER 3

METHODOLOGY

Rainfall-runoff models have been developed to understand and predict the catchment response to rainfall. The prediction of catchment response forms an important part of water resources management and it is of practical interest for the estimation of flood events. The complexity of runoff production processes that arises from the spatial heterogeneity in topography, soil characteristics, vegetation covers and antecedent moisture conditions has been represented in distributed hydrological models. The distributed models have to handle large amount of data. The development of the GIS software has enabled the hydrologists to study the spatially distributed catchment characteristics and their influence on runoff generation.

The model described here is spatially distributed unit hydrograph which is similar to the concept of geomorphic instantaneous unit hydrograph except that GIS is used to describe the connectivity of the links in the watershed flow network, which eliminates the need for using probability arguments to combine the movement of water through the links. Moreover, the GIS-based approach permits the spatial pattern of effective rainfall to vary by isochrone zones within the watershed, thus relaxing the requirement for uniform effective rainfall over the whole watershed.

3.1 Determination of effective rainfall

Effective rainfall is that rainfall which starts flow over the land surface after meeting the losses. Effective rainfall becomes direct runoff at the outlet after draining out from the whole catchment. Determination of effective rainfall hyetograph is the important task in the study of rainfall-runoff relationships. The losses are determined by deducting the effective rainfall hyetograph from the observed rainfall hyetograph. The losses are calculated by two methods viz. infiltration equations and SCS CN method. The determination of effective rainfall for a storm event by SCS CN method is briefed in the following section.

3.1.1 SCS CN method

The runoff curve number method is a procedure for computing hydrologic abstraction from storm rainfall developed by the USDA Soil Conservation Service. In this method, runoff depth (i.e., effective rainfall depth) is a function of total rainfall depth and an abstraction parameter referred to as runoff curve number, curve number, or CN. The curve number varies in the range 1 to 100, being a function of runoff producing catchment properties viz. hydrologic soil type, land use and treatment, ground surface condition, and antecedent moisture condition (AMC). The runoff curve number method was developed based on 24-h rainfall-runoff data.

For a storm event, the depth of effective rainfall or direct runoff P_e is less than or equal to the depth of total rainfall P . After runoff begins, the depth of water retained in the catchment F_a is less than or equal to the potential maximum retention S . There is some amount of rainfall I_a (initial abstraction before ponding) for which no runoff will occur, so the potential runoff is $P - I_a$.

The hypothesis of the SCS method (Soil Conservation Service, 1972) is based on the assumption of proportionality between retention and runoff:

$$\frac{F_a}{S} = \frac{P_e}{P - I_a} \quad \text{.....1}$$

which states that the ratio of actual retention to potential retention is equal to the ratio of actual runoff to potential runoff. This assumption underscores the conceptual basis of the runoff curve number method.

From the continuity principle

$$P = P_e + I_a + F_a \quad \text{.....2}$$

Combining equations 1 and 2 to solve for P_e gives

$$P_e = \frac{(P - I_a)^2}{P - I_a + S} \quad \text{for } P > I_a \quad \text{.....3}$$

which is the basic equation for computing the depth of effective rainfall or direct runoff from a storm event.

An empirical relation was developed from the study of results from many small experimental watersheds.

$$I_a = 0.2S \quad \text{.....4}$$

Substituting the value of I_a in the equation 3 to get the following equation

$$P_e = \frac{(P - 0.2S)^2}{P + 0.8S} \quad \text{.....5}$$

The standard initial abstraction coefficient recommended by SCS is 0.2. Springer et al. (1980) evaluated small humid and semiarid catchments and they found that the coefficient in Equation 4 varied in the range 0.0 to 2.6. For research applications and particularly when warranted by field data, it is possible to consider the initial abstraction coefficient as an additional parameter in the runoff curve number method.

In metric units, the curve number and S are related by

$$S = \frac{2540}{CN} - 25.4 \quad \text{.....6}$$

where S is in cm.

Tables of runoff curve numbers for various hydrologic soil-cover complexes are widely available. The hydrologic soil-cover complex describes a specific combination of hydrologic soil group, land use and treatment, hydrologic surface condition, and antecedent moisture condition.

Hydrologic Soil Group

All soils are (Soil Conservation Service, 1972) classified into four hydrologic soil groups of distinct runoff producing properties. These groups are labelled as A, B, C, and D.

Group A consists of soils of low runoff potential, having high infiltration rates even when wetted thoroughly. They are primarily deep, very well drained sands and gravels, with a characteristically high rate of water transmission.

Group B consists of soils with moderate infiltration rates when wetted thoroughly, primarily moderately deep to deep, moderately drained to well drained, with moderately fine to moderately coarse textures. These soils have a moderate rate of water transmission.

Group C consists of soils with slow infiltration rate when wetted thoroughly, primarily soils having a layer that impedes downward movement of water or soils of moderately fine to fine texture. These soils have a slow rate of water transmission.

Group D consists of soils of high runoff potential, having very slow infiltration rates when wetted thoroughly. They are primarily clay soils with high swelling potentials, soils with a permanent high water Table, soils with a clay layer near the surface, and shallow soils overlying impervious material. These soils have a very slow rate of water transmission.

Land use and Treatment

The effect of the surface condition of a watershed is evaluated by means of land use and treatment classes. Land use pertains to the watershed cover, including every kind of vegetation, litter and mulch, fallow (bare soil), as well as non-agricultural uses such as water surfaces (lakes, swamps, etc.), impervious surfaces (roads, roofs, etc.), and urban areas. Land treatment applies mainly to agricultural land uses, and it includes mechanical practices such as contouring or terracing and management practices such as grazing control and crop rotation. A class of land use/treatment is a combination often found in a catchment.

The runoff curve number method distinguishes between cultivated land, grasslands, and woods and forests. For cultivated lands, it recognises the following land uses and treatments: fallow, row crop, small grain, close-seed legumes, rotations (from poor to good), straight-row fields, contoured fields, and terrace fields.

Hydrologic Condition

Grasslands are evaluated by the hydrologic condition of native pasture. The percent of areal coverage by native pasture and the intensity of grazing are visually estimated. A poor hydrologic condition describes less than 50 percent areal coverage and medium grazing. A good hydrologic condition describes more than 75 percent areal coverage and light grazing.

The hydrologic condition of woods is visually estimated as follows: (1) poor-heavily grazed or regularly burned woods, with very little litter and few shrubs, (2) fair-grazed but not burned, with moderate litter and some shrubs, and (3) good-protected from grazing, with heavy litter and many shrubs covering the surface.

Antecedent Moisture Condition

The runoff curve number method has three levels of antecedent moisture, depending on the total rainfall in the 5-d period preceding a storm. The AMC can be estimated from Table 1 or other similar regionally derived tables.

Table 2(a) shows runoff curve numbers for urban areas, Table 2(b) shows them for cultivated agricultural areas, Table 2(c) shows them for other agricultural lands, and Table 2(d) shows them for arid and semiarid range lands. Runoff curve numbers shown in these Tables are for the average AMC II condition. For dry conditions (AMC I) or wet conditions (AMC III), equivalent curve numbers can be computed by

$$CN(I) = \frac{4.2CN(II)}{10 - 0.058CN(II)} \quad \dots\dots 7$$

$$CN(III) = \frac{23CN(II)}{10 + 0.13CN(II)} \quad \dots\dots 8$$

The primary advantages of the curve number method are simple, predictable, stable, and is supported by empirical data. The disadvantages are as follows:

- * Originally developed using regional data, mostly from the midwest of USA (it is recommended to use regional CN values where available).
- * The method may be very sensitive to CN and AMC, particularly for the lower CNs and/or rainfall depths. It is lack of clear guidance on how to vary AMC.
- * The method is best for agricultural sites. It rates fairly when applied to range sites and generally does poorly on forest sites. It does better on sites with negligible base flow (e.g., ephemeral streams in arid and semi-arid regions).
- * The method fixes the initial abstraction at 0.2S (0.2 of the potential retention by the watershed). The initial abstraction, however, could be interpreted as a regional

parameter that could be used to improve the method's performance. Insufficient research exists to permit a conclusion on this point.

3.2 The Eight Directional Cell Flow Model

All GRID based GIS systems contain routines which determine flow direction over land surface terrain using the eight-directional cell flow model (the pour point model). Water on grid cell is permitted to flow to one of its eight nearest neighbour cells as shown in Figure1a. By taking a grid of terrain elevations (Figure1b), determining the slope of the line joining each cell with each of its neighboring cells, a grid of flow directions is created with one direction for each cell which represents the direction of steepest descent among the eight permitted choices. This grid is shown in Figure1c as a set of arrows but in fact is stored in GIS as a grid of numbers where each flow direction has a unique identifying number. Equivalent one directional flow network is constructed by connecting the cell centers as shown in Figure1d. Two-dimensional spatially distributed processes such as precipitation and infiltration can be modeled using the grid and the runoff from them can be routed to the watershed outlet through the associated one-dimensional flow network.

3.3 Flow routing in the cell

The flow accumulation in a grid cell is presented in Figure 2. The cells in the boundary of the catchment or the cells with the zero flow accumulation value have only the overland flow. The flow accumulation in the cell as represented by the figure is calculated as follows:

$$Q = Q_1 + Q_2 + q \quad \dots\dots\dots 9$$

here Q_1 is the flow from the immediate upstream cell, Q_2 is the flow from the upstream corner cell and q is the locally generated flow. In-built algorithm is available to calculate the flow in each cell in all standard GIS packages.

3.4 Calculation of travel time

The overland flow runoff generated from cell area A is $q = Ai_e$ where i_e is the average effective rainfall intensity computed by the Soil Conservation Service (SCS)

runoff curve number method. A curve number is assigned to each cell by SCS CN method on the basis of landuse and soil type and is stored in GIS database. Each cell thus generates an effective rainfall depending on its CN value, resulting in a spatially distributed effective rainfall within the watershed boundary.

3.4.1 Overland flow travel time

The overland flow travel time is computed as the time to steady flow given by the kinematic wave equation (Chow et al., 1988).

$$t_c = \frac{L^{0.6} n^{0.6}}{i_e^{0.4} S_x^{0.3}} \quad \dots\dots 10$$

where L is the length of the overland flow, n is the Manning roughness coefficient and S_x is the land slope.

3.4.2 Travel times in the channel

The average flow velocity, V, through a channel is computed by combining the Manning and continuity equations (Chow et al, 1988) for a wide channel, written respectively as

$$V = \frac{S_0^{1/2}}{n} y^{2/3} \quad \dots\dots 11$$

and

$$Q = VBy \quad \dots\dots 12$$

into one equation for velocity (Muzik, 1996), given by

$$V = \left[\frac{S_0^{1/2}}{n} \left(\frac{Q}{B} \right)^{2/3} \right]^{3/5} \quad \dots\dots 13$$

where S₀ is the grid slope determined by the digital elevation model, y is the depth of flow, Q is the discharge and B is the channel width.

The travel time in the channel is computed using the equation 13 as follows:

$$t = \frac{L}{V} \quad \dots\dots 14$$

where L is the channel length and V is the velocity in each grid cell.

3.5 Time-Area diagram

Velocity is a vector quantity specified by magnitude and direction. It is represented by Figure 3a. The velocity magnitudes for channel cells are calculated by the equation 13. The travel time in the channel cell is calculated by the equation 14. The overland flow travel time in the boundary cells or the cells with zero flow accumulation is calculated by the equation 10. The grid of flow travel times where the value in each cell is the time taken for water from that cell to flow to the watershed outlet can be created by combining the grid of overland flow travel time and the channel flow travel time.

The cells may then be classified into zones i , $i = 1, 2, \dots$, whose travel time t falls in to time intervals Δt , that is, the zone 1 has travel time $0 \leq t < \Delta t$, the zone 2 has travel time $\Delta t \leq t < 2\Delta t$, and so on. The line bounding the outer limit of the cells in zone i is the isochrone of travel of time $t = i\Delta t$ to the watershed outlet. The total area of cells in zone i is A_i . In this way, the isochrone map of the watershed is created as shown in Figure 3b. The isochrone which has maximum time of flow to the outlet is the time of concentration of the watershed, t_c , also sometimes called the time of equilibrium.

The time-area diagram is a graph of cumulative drainage area flowing to the outlet within a specified time of travel. It is constructed by summing the incremental areas A_i as shown in Figure 4b. Thus at time points $t = 0, \Delta t, 2\Delta t, \dots, i\Delta t, \dots$, the cumulative area draining to the outlet $A(i\Delta t)$ is given by (Maidment, 1993) :

$$A(i\Delta t) = \sum_{k=1}^i A_k \quad \dots\dots 15$$

and conversely, the incremental area are given by (Maidment, 1993) :

$$A_i = A[i\Delta t] - A[(i-1)\Delta t] \quad \dots\dots 16$$

it is important to note that the incremental time-area diagram (Figure 4a) is a discrete time function having a single value over each time interval Δt , while the cumulative time-area diagram (Figure 4b) is a continuous time function whose sampled value is given at

regular time points by equation 15. Thus, if the time of flow grid into isochrones separated by a different time step Δt is classified, the appearance of the incremental time-area histogram will be altered but the cumulative time-area diagram will simply be the same continuous curve sampled with a different time step.

3.6 Distributed Unit hydrograph

The concept of a spatially distributed unit hydrograph, proposed by Maidment (1993), is based on the fact that the unit hydrograph ordinate at time $i\Delta t$ is given by the slope of the watershed time-area diagram over the interval $[(i-1)\Delta t, i\Delta t]$. The validity of the above can be proved by considering the S-hydrograph method. An S-hydrograph, defined as the runoff at the outlet of a watershed resulting from a continuous effective rainfall occurring at rate i_e over the watershed, is given by

$$Q_S(i\Delta t) = i_e A(i\Delta t) \quad \dots\dots 17$$

where $A(i\Delta t)$ is the watershed area contributing to flow $Q_S(i\Delta t)$ at the outlet at time $i\Delta t$. The direct runoff hydrograph discharge at time $i\Delta t$, resulting from a pulse of effective rainfall $P_e = i_e\Delta t$, is equal to the difference between the S-hydrograph value at time $i\Delta t$ and its value lagged by time Δt , i.e.

$$Q_D(i\Delta t) = i_e A(i\Delta t) - i_e A[(i-1)\Delta t] \quad \dots\dots 18$$

The unit hydrograph ordinates are $U(i\Delta t) = Q_D(i\Delta t)/P_e$, and thus

$$U(i\Delta t) = \frac{A(i\Delta t) - A[(i-1)\Delta t]}{\Delta t} \quad \dots\dots 19$$

or by

$$U_i = U(i\Delta t) = \frac{A_i}{\Delta t} \quad \dots\dots 20$$

Thus the unit hydrograph can be constructed by standard S-hydrograph method (Chow et al., 1988), i.e., the time-area curve is lagged by one hour and subtracted from original curve. The discharge values obtained, adjusted for unit input, yield the one-hour distributed unit hydrograph. The typical distributed unit hydrograph is presented in Figure 4c.

3.7 Direct Runoff Hydrograph

The portion of the rainfall, which produces direct runoff, is called the effective rainfall. This can be computed by SCS CN method as explained in the first section. The effective rainfall values are symbolized by $P_{e1}, P_{e2}, \dots, P_{ei}, \dots$, where P_e is the effective rainfall in mm and the corresponding direct runoff values are given by $Q_1, Q_2, \dots, Q_n, \dots$, where Q is a discharge rate at the watershed outlet measured in cumec. Given the effective rainfall hyetograph for a watershed, the direct runoff hydrograph is computed for the first time interval as (Maidment, 1993) :

$$Q_1 = P_{e1}U_1 \quad \dots\dots 21$$

and by substitution of $U_1 = A_1/\Delta t$ modifies above equation as follows (Maidment, 1993) :

$$Q_1 = \frac{P_{e1}A_1}{\Delta t} \quad \dots\dots 22$$

Thus, if an effective rainfall of intensity $P_{e1}/\Delta t$ begins falling on the watershed at time 0, after time Δt area A_1 is contributing to flow at the outlet so the direct runoff rate is $(P_{e1}/\Delta t)A_1$ at that time. After time $t = 2\Delta t$, there are two rainfall pulses to contend with P_{e1} and P_{e2} , and direct runoff is computed by (Maidment, 1993) :

$$\begin{aligned} Q_2 &= P_{e2}U_1 + P_{e1}U_2 \\ &= \frac{1}{\Delta t} [P_{e2}A_1 + P_{e1}A_2] \end{aligned} \quad \dots\dots 23$$

which include the immediate impact at the outlet of P_{e2} flowing from area A_1 plus the delayed effect of P_{e1} flowing from area A_2 . In normal unit hydrograph calculations, the effective rainfall is assumed uniformly distributed over the watershed in space so that any particular rainfall increment P_{ej} refers to the average rainfall in time interval $[(j-1)\Delta t, j\Delta t]$ on all areas $A_1, A_2, \dots, \text{etc.}$

With GIS grid capabilities for rainfall mapping, this uniform spatial rainfall distribution is no longer necessary so that two subscripts are needed to characterize rainfall, P_{eij} , where P_{eij} is the average effective rainfall over all cells in isochrone zone i during time interval j . Direct runoff at time $t = n\Delta t$ is given by summing the runoff contributions from each of the applicable isochrone zones suitably lagged in time (Maidment, 1993) :

$$Q_n = \sum_{i=1}^n \frac{P_{eij} A_i}{\Delta t} \quad \text{where } j = n-i+1 \quad \dots\dots 24$$

It has been decided to use SCS CN method to derive the effective rainfall hyetograph over the watershed in this study. The abstraction calculated by the SCS CN method includes both the retention and the infiltration and the method is simple to adopt. In this method, the effective rainfall is calculated by incorporating the soil moisture, landuse and soil properties. The in-built routines of eight-direction flow model of GIS ARC/INFO have been used to derive the links of watershed flow network. The velocity has been assigned to each grid of the watershed as explained in section 3.4. Time-area has been derived using the generated equivalent flow network as explained in the section 3.5. The spatially distributed unit hydrograph has been derived as explained in the section 3.6. The direct runoff hydrographs of the storms considered in this study have been calculated by convoluting the spatially distributed unit hydrograph with the effective rainfall hyetograph.

CHAPTER 4

THE STUDY AREA

4.1 The Kolar Basin

The Kolar sub-basin is located in the latitude range of 22° 40' to 23° 08' East and longitude 77° 01' to 77° 29' North. The Kolar river originates in the Vindhya mountain range at an elevation of 550 m above mean sea level (msl) in the district Sehore of Madhya Pradesh (M.P.) state. The river during its 100 km. Course first flows towards east and then towards south before joining the river Narmada near a place Neel Kanth. During the course, the Kolar river drains an area of about 1350 sq.km. In the present study only the catchment area of 863.125 sq.km. upto Satrana gauge-discharge site has been considered. The entire basin lies in two districts Sehore and Raisen.

Topographically, the Kolar basin can be divided into two distinct zones, i.e., upper four-fifth part and lower one-fifth part. The upper four-fifth part having elevations ranging from 600 m to 350 m is predominantly covered by deciduous forest (dense and open). The boundaries of catchment are mild sloped at the northern end of the basin. The river debauches to plains from this area upstream of Jholiapur through ramp shaped southward sloping topography. The soils are skeleton to shallow in depth except near channels where they are relatively deep. The rock outcrops are easily visible at many places. In this area, the rocks are weathered and deep fissures can be seen. The channel beds are rocky or gravel. The soils get saturated even during low intensity rains and water moves through the fissures rapidly. Agricultural activity is carried out in relatively large areas in the north western part (adjacent to Ichhwar) and in small pockets elsewhere in which the main crops are wheat and gram. The general response of this upper part of basin to rain appears to be quick.

The lower part of the basin consisting of flat bottomed valley narrowing towards the outlet and having elevations ranging from about 300 m to 350 m is predominantly cultivable area. The soils are deep in the area and have flat slopes. The places where agricultural activity is carried out have bunded fields in which water is impounded during

the monsoon period. The response of this area to input rainfall is likely to be quiet slow. Part of this area comes under the command of Kolar dam. The index map of Kolar Basin upto Satrana is presented in Figure 5. The detailed drainage map is presented in Figure 6.

4.2 Data Availability

The base map of the Kolar sub-basin was prepared using the Survey of India toposheets (No. 55 E/4, 8 and 55 F/1, 5, 6) at a scale of 1:50,000. Remote Sensing data in the form of false coloured composite (FCC) was available at NIH, Roorkee for the year 1989. For this study IRS LISS II data of Path/Row 27/52 and 28/51 of post monsoon season, 1989 were used for the classification of landuse. The pattern of reflectance was used to classify the landuse types. The spectral signatures of different landuse categories in the satellite imageries in FCC are given in Table 3. The landuse of the basin was classified according to the spectral signatures and is presented in Figure 7.

The soil map in a scale 1:250000 was obtained from the Narmada Valley Development Authority (NVDA). However, the hydraulic properties of the soils were not directly available and were derived from secondary sources. The upper portion of the basin consists of shallow black soil and the lower portion of the basin consists of deep black soil. According to these soil properties, two soil groups are classified and are hydrologic soil group 'C' and 'B' respectively. The soil map of the basin is presented in Figure 8.

Hourly rainfall data for the years 1983 to 1988 was available. Rainfall data at three stations i.e. Brijeshnagar, Birpur and Jholiapur were considered for this study. The Thiessen polygon for these rainfall stations was derived using the ARC/INFO facility and is presented in Figure 9. The rainfall events 19.8.1983, 09.08.1984, 30.07.1985, 13.08.1985, 14.08.1986 and 26.08.1987 were considered for the simulation of the hydrographs. The spatially averaged rainfall values for the events considered and the corresponding discharge at Satrana are presented in Table 4 and Table 5. The discharge values presented in Table 5 are direct runoff hydrograph. The base flow values are deducted from the total runoff hydrograph.

CHAPTER 5

DEVELOPMENT OF THE DISTRIBUTED MODEL

The modelling and forecasting of hydrological processes have been traditionally carried out through lumped models in order to include all information needed when simulating a quite complex natural system. Such a system behaviour is obviously the outcome of several interacting contributions usually averaged in space and time over an appropriate multidimensional domain. Effort has been made to the development of distributed hydrological models in order to overcome some of the traditional limitations of lumped modelling. The improvement of high performance artificial memories and computational resources makes the data handling capabilities of GIS able to analyse large quantities of distributed geographically referenced information. Many GIS softwares like ILWIS, ERDAS, GRASS, ARC/INFO, etc., are available. The unix version of GIS ARC/INFO (Ver. 7) was used to develop the distributed unit hydrograph as explained in the chapter 3. The PC version ARC VIEW was used to generate output maps as the composition of the map is easy in this software. In ARC/INFO GIS the map composition is done through set of commands or macro.

5.1 The ARC/INFO GIS

ARC/INFO Version 7 is a Geographic Information System with advance capabilities developed by Environmental Systems Research Institute, USA. ARC/INFO TIN, ARC/INFO NETWORK, ARC/INFO COGO AND ARC/INFO GRID are extensions to ARC/INFO. These extensions are provided to have advanced analysis in GIS. The ARC EDIT module was used to digitise the contour, landuse and soil maps and to correct these digitised maps to have them error free.

5.2 Generation of Input Grid Maps

The contour map at 20 m interval was prepared by tracing the contours from Survey of India toposheets (No. 55 E/4, 8 and 55 F/1, 5, 6) at a scale of 1:50,000 of Kolar basin upto Satrana. The spot heights were represented by small arcs. Then the traced map was scanned through a scanner and the scanned image was imported to the ERDAS

IMAGINE and the image was edited and georeferenced. The edited image was imported to GIS ARC/INFO and projected to real world co-ordinates. The contours were traced with the auto tracing facility of the GIS ARC/INFO and the elevation values were assigned to the contours. The contour map was used to generate the DEM of the Kolar Basin upto Satrana using TOPOGRIDTOOL command in ARC module of the GIS ARC/INFO software. The cell size of the DEM was selected as 250 m square. The sinks of the DEM were filled with the FILL command of the GRID module to have a error free DEM. The digital elevation model (DEM) is presented in Figure 10.

The error free DEM was used to generate the drainage flow network. The equivalent drainage network is presented in Figure 11. If the cells in Figure 1 have a size of 1 unit (250 m), flow between two adjacent cell centers in either the horizontal or vertical directions involves a distance of 1 unit (250 m) while flow between diagonal cell centers involves a distance of $\sqrt{2} = 1.414$ units (1.414*250 m). Beginning in Figure 1d with the cell adjacent to the watershed outlet (which has a flow distance of 0.5 units), calculations proceed cell by cell upstream along the flow network links, with the value stored in each cell being the flow distance to the outlet. This flow distance was later used to calculate the time of concentration in each cell.

The vector maps of the landuse, soil and Thiessen polygon were converted to raster maps of 250 m cell size using commands of ARC module. The overlay and spatial operations can be done efficiently in GRID module.

5.3 Calculation of Effective Rainfall

The cumulative abstractions can be calculated using the following equation (Chow et al, 1988):

$$F_a = \frac{S(P - I_a)}{P - I_a + S} \quad P \geq I_a \quad \dots\dots\dots 25$$

where F_a is cumulative abstractions, S is potential infiltration, I_a is initial abstraction and P is the cumulative rainfall.

The cumulative excess rainfall can be calculated by the following equation:

$$P_e = P - I_a - F_a \quad \dots\dots 26$$

where P_e is the cumulative excess rainfall.

The curve number was assigned by interpreting the landuse and soil for antecedent moisture condition (AMC) II from the Tables 1, 2a, 2b, 2c and 2d. The assigned curve numbers for different landuse and soil group are presented in Table 6 and Figure 12. The total rainfall excess for each storm event considered for the simulation through distributed unit hydrograph was calculated from dividing the total volume of the storm event by total drainage area. The initial abstractions for each storm were adjusted according to total excess rainfall by trial and error method and are presented in Table 7. Springer et al (1980) evaluated the value of initial abstraction for small humid and semiarid catchments and found that it varied in the range 0.0 to 2.6.

The potential infiltration was calculated using the equation 6 and the curve number values are presented in the Table 6. The cumulative abstraction was calculated by using equation 25 and the cumulative rainfall excess was calculated by the equation 26 for each time interval of the cumulative rainfall. The rainfall excess hyetograph for a particular time interval was calculated from deducting the cumulative rainfall excess of the previous time interval. The rainfall excess hyetograph for the storm events are presented in Table 8.

5.4 Derivation of Time-Area Diagram

A largest block of rainfall intensity was applied uniformly over whole basin. Using equations 5 and 6, and the curve numbers assigned, the rainfall excess generated from each cell was calculated. The rainfall excess generated from each cell is different on the basis of the curve number and thus resulting in a spatially distributed excess rainfall within the watershed boundary. The rainfall excess in each cell multiplied by the area of the cell (250 m) gave the local flow from the cell. The local flow values were accumulated from upstream to get the discharge at the outlet of the basin. The outlet of the basin was determined by the BASIN command of the GRID module. The

accumulated flow in each cell was used in the equation 13 to calculate the velocity in each cell with slope, Manning's n and width of the channel. The bed width of the channels at some locations are available and are 60 m, 13 m, 7.5 m at Satrana, Khamkhera and Bamladhar respectively. The same values were used to assume the average channel width in flooding condition with flow accumulation values in the cells. The average channel width in the main channel was assumed to be varied between 110m and 130 m. The other channel widths assumed were 110 m, 40 m, 1 m where the flow accumulation values were 4100, 100, 0 respectively. This indicates that each cell contains a channel. In ARC/INFO GIS the flow accumulation in the boundary cell is zero since the flow into the cell is zero. The Manning's n were assigned according to landuse and are presented in Table 9. The slope in the cells was considered to be 0.5 per cent where the value was less than 0.5 per cent. 4756 cells with the slope less than 0.5 per cent were present. Total cells present in the map were 13810. The slope map of the basin is presented in Figure 13. The flow length divided by the velocity in each cell gave the time of concentration in each cell. The incremental drainage area against the unit interval of time of concentration (1 hour) was compiled as explained in the section 3.5 and is presented in Table 10. The isochrone map of the basin is presented in Figure 14. The time-area diagram (S-curve) was derived by adding the incremental drainage area and is presented in Figure 15.

5.5 Determination of Direct Runoff Hydrograph

The distributed hydrograph was derived by applying the standard S-hydrograph method (Chow et al, 1988) i.e., the time-area curve was lagged by 1 hour and was subtracted from the original curve. The distributed unit hydrograph is presented in Figure 16. This distributed unit hydrograph was convoluted with the rainfall excess hyetograph to get the direct runoff hydrograph for all the storm events as explained in the section 3.7. The simulated direct runoff values are presented in Table 11. The zero values were calculated according to the observed time period for the purpose of comparison.

CHAPTER 6

DISCUSSION OF RESULTS

The runoff hydrographs were simulated as explained in the previous chapter using the storm events. The simulated runoff hydrographs with the corresponding observed runoff hydrograph are presented in Figures 17, 18, 19, 20, 21, and 22. The errors of the observed peak discharge with the simulated peak discharge and the errors of the observed time to peak flow with the simulated time to peak flow were computed and are presented in Table 12.

In the simulation of storm event 1, it was observed that the observed flow was matching with the simulated flow upto the 5th hour and was slowly increasing till the peak as compared to the observed flow hydrograph. The peak of the simulated hydrograph was at the 16th hour from the beginning of the storm whereas the observed peak was at the 11th hour from the beginning of the storm. The recession limb of the simulated hydrograph was lower than the recession limb of the observed hydrograph after the 26th hour from the beginning of the storm. The error of observed peak flow discharge with the simulated peak flow discharge was 19.62 per cent.

In the simulation of storm event 2, it was observed that the observed flow was not matching with the simulated flow right from the beginning of the storm to its end. The peak of the simulated hydrograph was at the 14th hour from the beginning of the storm whereas the observed peak was at the 10th hour from the beginning of the storm. The error of observed peak flow discharge with the simulated peak flow discharge was 0.89 per cent.

In the simulation of storm event 3, it was observed that the simulated flow was above the observed flow upto the 12th hour from the beginning of the storm. The value of simulated peak flow was less than the observed peak flow. The peak of the simulated hydrograph as well as the observed peak was at the 16th hour from the beginning of the storm. The recession limb of the simulated hydrograph was matching with the recession

limb of the observed hydrograph after the 28th hour from the beginning of the storm. The error of observed peak flow discharge with the simulated peak flow discharge was 8.32 per cent.

In the simulation of storm event 4, it was observed that the simulated flow was not matching with the observed flow right from the beginning of the till to its end. The value of simulated peak flow was much lower than the observed peak flow. The peak of the simulated hydrograph was at the 9th hour from the beginning of the storm whereas the observed peak was at the 5th hour from the beginning of the storm. The recession limb of the simulated hydrograph was lower than the recession limb of the observed hydrograph. The error of observed peak flow discharge with the simulated peak flow discharge was 20.87 per cent.

In the simulation of storm event 5, it was observed that the simulated flow was not matching with the observed flow right from the beginning of the till to its end. The value of simulated peak flow was much higher than the observed peak flow. The peak of the simulated hydrograph was at the 15th hour from the beginning of the storm whereas the observed peak was at the 14th hour from the beginning of the storm. The recession limb of the simulated hydrograph was lower than the recession limb of the observed hydrograph upto the 27th hour from the beginning of the storm. The error of observed peak flow discharge with the simulated peak flow discharge was 26.00 per cent.

In the simulation of storm event 6, it was observed that the simulated flow was not matching with the observed flow right from the beginning of the till to its end. The value of simulated peak flow was lower than the observed peak flow. The peak of the simulated hydrograph was at the 14th hour from the beginning of the storm whereas the observed peak was at the 13th hour from the beginning of the storm. The recession limb of the simulated hydrograph was higher than the recession limb of the observed hydrograph upto the 23rd from the beginning of the storm. The error of observed peak flow discharge with the simulated peak flow discharge was 9.77 per cent.

The matching of the observed hydrograph with the simulated hydrograph was observed to be fair in the case of storm events 3 and 6. The percentages of error in peak discharge were from 0.89 to 26. The percentages of error in time to peak were from 0 to 80. The high percentage of error in the event no. 2 and 4 is due to the following reasons:

1. The observational errors.
2. The assumptions made in the derivation of time-area diagram.
3. The consideration of storm movement is avoided in the calculation of effective rainfall hyetograph.
4. The approximation of land use map from the FCC of a fixed date.

CHAPTER 7

CONCLUSIONS

The one-hour distributed hydrograph was determined for Kolar Basin using S hydrograph technique from the time-area diagram of the basin. The time-area diagram was developed by compiling the time of concentration of unit incremental interval (1 hour) against the drainage area. The time of concentration was determined by dividing the flow length with flow velocity of the basin. The error free DEM created by ARC/INFO GIS was used to generate the drainage flow network. It was assumed that every cell in the DEM contains a channel. The flow velocity in the basin was computed by the derived equation by combining the Continuity and Manning's equations. The values of Manning's n were assumed according to the landuse. The channel width in flooding condition was assumed on the basis of available details of bed width of the channels at some locations. The curve numbers were assigned according to the landuse and soil type. The largest rainfall intensity block was applied uniformly over the basin to generate different rainfall intensity in each cell according to the curve number assigned and thus resulting in a spatially distributed rainfall excess. The accumulated discharge computed from spatially distributed rainfall excess in each cell was used in the derived equation to find the flow velocity in each cell.

Six rainfall storm events were considered for the simulation of direct runoff hydrographs. Those were 19.08.1983, 09.08.1984, 30.07.1985, 13.08.1985, 14.08.1986 and 26.08.1987. The rainfall excess hyetographs for all these storms were computed by the deducting the cumulative abstraction and the initial abstraction from the cumulative rainfall. The rainfall excess hyetographs were convoluted with the one-hour unit distributed hydrograph to derive the direct runoff hydrographs.

The percentages of error of the observed peak flow with the simulated peak flow and the observed time to peak with the simulated time to peak for all storms were computed. It was observed that the errors of peak flow varied from 0.89 per cent to 25.07 percent and the errors of time to peak varied from 0 to 80 percent. The matching of the

observed hydrograph with the simulated hydrograph was observed to be fair in the case of storm events 3 and 6. The errors in the peak discharge and time to peak can be reduced by introducing an algorithm to route the flow in each cell to get an attenuated flow at the outlet of the basin.

This type of distributed unit hydrograph can be developed for any ungauged catchment without rainfall and runoff data since the development involves watershed hydraulics. The derived unit hydrograph can be used to get the direct runoff hydrograph by convoluting the rainfall excess hyetograph. A common velocity will be developed for any intensity of rainfall on the basis of this methodology. In reality, the velocity field depends on the intensity of rainfall. A proper methodology should be evolved to incorporate the effect of intensity of rainfall. The error may be introduced in the simulation of runoff by assuming the point rainfall as distributed one by the Thiessen polygon method.

REFERENCES

1. Ahmad, Tanveer.(1996). "Catchment modelling in GIS environment". M.E. Thesis, Department of Hydrology, University of Roorkee, Roorkee, India, 247667.
2. Barbera, P.L.A, Lanza, L., and Siccardi, F. (1993). "Hydrologically Oriented GIS and Application to Rainfall-Runoff Distributed Modelling: case study of the Arno basin". *HydroGIS 93: Application of Geographic Information Systems in Hydrology and Water Resources (Proceedings of the Vienna Conference)*, IAHS Publ. No. 211, 171-179.
3. Beston, R.P. (1964). "What is watershed runoff?" *Journal of Geophysical Research*, 69(8), 1541-1522.
4. Chow, V.T., Maidment, D.R., and Mays, L.W., (1988). *Applied Hydrology*, McGraw Hill Book Company, New York.
5. Clark, C.O. (1945). "Storage and the Unit Hydrograph". *Transactions of the American Society of Civil Engineers*, Vol. 110, 1419-1446.
6. Correia, F.N., Rego, F.C., Saraiva, M.G., and Ramos, I. (1998). "Coupling GIS with Hydrologic and Hydraulic Flood Modelling". *Water Resources Management*, 12, 229-249.
7. Dooge, J.C.I. (1959). "A General Theory of the Unit Hydrograph". *Journal of Geophysical Research*, 64(1), 241-256.
8. Jain, M.K., and Seth, S.M. (1997). "Rainfall-Runoff Modelling of a Himalayan Catchment using a Distributed Approach". *Institution of Engineers (India) Journal*, Vol. 78, 89-92.
9. Maidment, D.R. (1993). "Developing a Spatially Distributed Unit Hydrograph by using GIS". *HydroGIS 93: Application of Geographic Information Systems in Hydrology and Water Resources (Proceedings of the Vienna Conference)*, IAHS Publ. No. 211, 181-192.
10. Maidment, D.R., Olivera, F., Calver, A., Eatherall, A., and Fraczek, W. (1996). "Unit Hydrograph Derived from a Spatially Distributed Velocity Field". *Hydrological Processes*, Vol. 10, 831-844.

11. Molnar, D.K., and Julien, P.Y. (1998). "Grid-Size Effects on Surface Runoff Modelling". *Journal of Hydrologic Engineering*, ASCE, 5(1), 8-16.
12. Muzik, I. (1996). "Flood Modelling with GIS-Derived Distributed Unit Hydrographs". *Hydrological Processes*, Vol. 10, 1401-1409.
13. Nash, J.E. (1957). "The Form of the Instantaneous Unit Hydrograph". *IAHS Publication no. 45*, 3-4, 114-121.
14. Polarski, M. (1997). "Distributed Rainfall - Runoff Model Incorporating Channel Extension and Gridded Digital Maps". *Hydrological Processes*, Vol. 11, 1-11.
15. Ponce, V.M. (1989). *Engineering Hydrology, Principles and Practices*, Prentice Hall, Englewood Cliffs, New Jersey 07632.
16. Rodriguez-Iturbe, I., and Valdes, J.B. (1979). "The Geomorphological Structure of Hydrologic Response". *Water Resources Research*, 15(6), 1409-1420.
17. Soil Conservation Service (1972), *National Engineering Handbook, Section 4, Hydrology*, U.S. Department of Agriculture, Washington, D.C.
18. Springer, E.P., McGurk, B.J., Hawkins, R.H., and Coltharp, G.B. (1980). "Curve numbers from watershed data". *Symposium on Watershed Management*, ASCE, Boise, Idaho, 938-950.
19. *Understanding GIS, The ARC/INFO Method (Version 7.03)* (1992). ESRI, Redlands, ISBN:1-879102-07-2.

Table 1 Seasonal Rainfall Limits for Three Level of Antecedent Moisture condition (AMC)

AMC	Total 5-d Antecedent Rainfall (cm)	
	Dormant season	Growing season
I	Less than 1.3	Less than 3.6
II	1.3 to 2.8	3.6 to 5.3
III	More than 2.8	More than 5.3

Note: This table was developed using data from the midwestern United States. Therefore, caution is recommended when using the values supplied in this table for AMC determinations in other geographic or climatic regions.

Table 2(a) Runoff Curve Number for Urban areas¹

Cover Description	Average Percent Impervious area ²	Curve Numbers for Hydrologic Soil Group:			
		A	B	C	D
<i>Fully developed urban areas (vegetation established)</i>					
Open space (lawns, parks, golf courses, cemeteries, etc.) ³ :					
Poor condition (grass cover less than 50 %)		68	79	86	89
Fair condition (grass cover 50 to 75 %)		49	69	79	84
Good condition (grass cover greater than 75 %)		39	61	74	80
Impervious areas:					
Paved parking lots, roofs, driveways, etc. (excluding right-of-way)		98	98	98	98
streets and roads:					
Paved; curves and storm sewers (excluding right-of-way)		98	98	98	98
Paved; open ditches (including right-of-way)		83	89	92	93
Gravel (including right-of-way)		76	85	89	91
Dirt (including right-of-way)		72	82	87	89
Western desert urban areas:					
Natural desert landscaping (pervious areas only) ⁴		63	77	85	88
Artificial desert landscaping (impervious weed barrier, desert shrub with 1- to 2-in. sand or gravel mulch and basin borders)		96	96	96	96
Urban districts:					
Commercial and business	85	89	92	94	95
Industrial	72	81	88	91	93
Residential districts by average lot size:					
$\frac{1}{8}$ ac. or less (town houses)	65	77	85	90	92
$\frac{1}{4}$ ac.	38	61	75	83	87
$\frac{1}{3}$ ac.	30	57	72	81	86
$\frac{1}{2}$ ac.	25	54	70	80	85
1 ac.	20	51	68	79	84
2 ac.	12	46	65	77	82
<i>Developing urban areas</i>					
Newly graded areas (pervious areas only, no vegetation) ⁵		77	86	91	94
Idle lands (curve numbers (CNs) are determined using cover types similar to those in Table 2 (c)).					

Notes:

¹Average antecedent moisture condition and $I_a = 0.25$

²The average percent impervious area shown was used to develop the composite CNs. Other assumptions are as follows: Impervious areas are directly connected to the drainage system; impervious areas have a $CN = 98$; and pervious areas are considered equivalent to open space in good hydrologic condition. CNs for other combinations may be computed using Figs. 5-17 or 5-18 of V. M. Ponce (1989).

³CNs shown are equivalent to those of pasture. Composite CNs may be computed for other combinations of open space cover type.

⁴Composite CNs for natural desert landscaping should be computed using Figs. 5-17 or 5-18 of V. M. Ponce (1989) based on the impervious area percentage ($CN=98$) and the pervious area CN. The pervious area CNs are assumed equivalent to desert shrub in poor hydrologic condition.

⁵Composite CNs to use for the design of temporary measures during grading and construction should be computed using Figs. 5-17 or 5-18 of V. M. Ponce (1989), based on the degree of development (impervious area percentage) and the CNs for the newly graded pervious areas.

Table 2(b) Runoff Curve Numbers for Cultivated Agricultural lands¹

Cover Description			Curve Numbers for Hydrologic Soil Group:				
Cover Type	Treatment ²	Hydrologic Condition ³	A	B	C	D	
Fallow	Bare Soil	-	77	86	91	94	
	Crop residue cover (CR)	Poor	76	85	90	93	
		Good	74	83	88	90	
Row crops	Straight row (SR)	Poor	72	81	88	91	
		Good	67	78	85	89	
	SR + CR	Poor	71	80	87	90	
		Good	64	75	82	85	
	Contoured (C)	Poor	70	79	84	88	
		Good	65	75	82	86	
	C + CR	Poor	69	78	83	87	
		Good	64	74	81	85	
	Contoured and terraced (C&T)	Poor	66	74	80	82	
		Good	62	71	78	81	
		Poor	65	73	79	81	
	C&T + CR	Good	61	70	77	80	
		SR	Poor	65	76	84	88
			Good	63	75	83	87
	Small grain	SR + CR	Poor	64	75	83	86
Good			60	72	80	84	
C		Poor	63	74	82	85	
		Good	61	73	81	84	
C + CR		Poor	62	73	81	84	
		Good	60	72	80	83	
C&T		Poor	61	72	79	82	
		Good	59	70	78	81	
C&T + CR		Poor	60	71	78	81	
		Good	58	69	77	80	
		SR	Poor	66	77	85	89
Good			58	72	81	85	
Close-seeded or broadcast legumes or rotation meadow	C	Poor	64	75	83	85	
		Good	55	69	78	83	
	C&T	Poor	63	73	80	83	
		Good	51	67	76	80	

Notes:

¹Average antecedent moisture condition and $I_a = 0.2S$.

²Crop residue cover applies only if residue is on at least 5 % of the surface throughout the year.

³Hydrologic condition is based on combination of factors that affect infiltration and runoff, including: (1) density and canopy of vegetated areas; (2) amount of year-round cover; (3) amount of grass or close-seeded legumes in rotation; (4) percent of residue cover on the land surface (good hydrologic condition is greater than or equal to 20 %); and (5) degree of surface roughness. *Poor*: Factors impair infiltration and tend to increase runoff. *Good*: Factors encourage average and better than average infiltration and tend to decrease runoff.

Table 2 (c) Runoff Curve Numbers for Other Cultivated Agricultural lands¹

Cover Description		Curve Numbers for Hydrologic Soil Group:				
Cover Type	Hydrologic Condition	A	B	C	D	
Pasture, grassland, or range-continuous forage for grazing ²	Poor	68	79	86	89	
	Fair	49	69	79	84	
	Good	39	61	74	80	
Meadow-continuous grass, protected from grazing and generally mowed for hay	-	30	58	71	78	
	Brush-brush-weed grass mixture with brush being the major element ³	Poor	48	67	77	83
		Fair	35	56	70	77
Good		30 ⁴	48	65	73	
Woods-grass combination (orchard or tree farm) ⁵	Poor	57	73	82	86	
	Fair	43	65	76	82	
	Good	32	58	72	79	
Woods. ⁶	Poor	45	66	77	83	
	Fair	36	60	73	79	
	Good	30 ⁴	55	70	77	
Farmsteads-buildings, lanes, driveways, and surrounding lots.	-	59	74	82	86	

Notes:

¹Average antecedent moisture condition and $I_a = 0.2S$.

²Poor: less than 50 % ground cover on heavily grazed with no mulch.

Fair: 50 to 75 % ground cover and not heavily grazed.

Good: more than 75 % ground cover and lightly or only occasionally grazed.

³Poor: less than 50 % ground cover.

Fair: 50 to 75 % ground cover.

Good: more than 75 % ground cover.

⁴Actual curve number is less than 30; use $CN = 30$ for runoff computations.

⁵CNs shown were computed for areas with 50 % woods and 50 % grass (pasture) cover. Other combinations of conditions may be computed from the CNs for woods and pasture.

⁶Poor: Forest litter, small trees, and brush are destroyed by heavy grazing or regular burning.

Fair: Woods are grazed but not burned and some forest litter covers the soil.

Good: Woods are protected from grazing, and litter and brush adequately cover the soil.

Table 2(d) Runoff Curve Numbers for Arid and Semiarid Rangelands¹

Cover Description		Curve Numbers for Hydrologic Soil Group:			
Cover Type	Hydrologic Condition ²	A ³	B	C	D
Herbaceous-mixture of grass, weeds, and low-growing brush, with brush the minor element.	Poor		80	87	93
	Fair		71	81	89
	Good		62	74	85
Oak-aspen-mountain brush mixture of oak brush, aspen, mountain mahogany, bitter brush, maple, and other brush.	Poor		66	74	79
	Fair		48	57	63
	Good		30	41	48
Pinyon-juniper-pinyon, juniper, or both; grass understory.	Poor		75	85	89
	Fair		58	73	80
	Good		41	61	71
Sagebrush with grass understory.	Poor		67	80	85
	Fair		51	63	70
	Good		35	47	55
Desert shrub-major plants include saltbrush, greasewood, creosotebush, blackbrush, bursage, palo verde, mesquite, and cactus.	Poor	63	77	85	88
	Fair	55	72	81	86
	Good	49	68	79	84

Notes:

¹Average antecedent moisture condition and $I_a = 0.25$. For range in humid regions, use Table 2 (c).

²*Poor*: less than 30 % ground cover (litter, grass, and brush overstory).

Fair: 30 to 70 % ground cover.

Good: more than 70 % ground cover.

³Curve numbers for group A have been developed only for desert shrub.

Table 3 Spectral signature of different landuse categories

Sl.No.	Category	Colour on F.C.C.
1	Thick forests	Deep red
2	Thin forests	Red with mottling of yellow in some patches
3	Cultivated area	Red with dark blue patches in irrigated areas
4	Barren land	Yellow to light brown mottled with red and blue
5	Sandy/gravelly	Yellow to light brown mottled river bed with red and blue
6	River bed	Blue
7	Snow	White

Table 4 Spatially averaged rainfall data for the events considered for the simulation

Time in hours	Event 1 19.8.1983 16 th hour (mm)	Event 2 9.8.1984 21 st hour (mm)	Event 3 30.7.1985 16 th hour (mm)	Event 4 13.8.1985 17 th hour (mm)	Event 5 14.8.1986 17 th hour (mm)	Event 6 26.8.1987 21 st hour (mm)
1	0.783	2.049	6.055	0.618	0.689	1.566
2	1.994	1.754	19.100	15.092	5.091	2.752
3	3.680	6.097	10.245	25.648	13.529	2.204
4	30.472	8.120	4.639	6.476	15.795	4.426
5	31.823	5.773	10.223	1.181	9.562	3.719
6	25.190	9.194	11.419		3.160	5.145
7	19.361	12.747	6.486		5.033	7.449
8	19.740	9.824	5.382		10.727	16.640
9	18.810	15.979	14.108		18.260	3.991
10	20.477	9.489	22.812		12.026	6.448
11	19.077	9.646	19.352		24.203	11.037
12	30.194	15.181	10.887		24.116	16.702
13	31.474	6.861	8.699		9.294	8.590
14	25.961	4.439	3.487		0.000	4.730
15	46.234	0.744	1.667		0.366	
16	8.522	0.142	3.947		0.244	
17	6.561	1.481	1.776		0.039	
18	2.857	2.342			0.566	
19	5.326	2.515			1.870	
20	2.797	0.366			0.078	
21	0.333					

Table 5 The observed discharge data (minus base flow) at Satrana for the events considered for the simulation

Time in hours	Event 1 19.8.1983 16 th hour (cumecs)	Event 2 9.8.1984 21 st hour (cumecs)	Event 3 30.7.1985 16 th hour (cumecs)	Event 4 13.8.1985 17 th hour (cumecs)	Event 5 14.8.1986 17 th hour (cumecs)	Event 6 26.8.1987 21 st hour (cumecs)
1	0.000	1.950	0.000	0.000	0.000	0.000
2	0.000	1.760	0.000	0.000	0.000	0.000
3	0.000	10.350	0.000	0.000	0.000	0.000
4	1.340	56.440	0.000	0.160	0.000	0.110
5	17.210	96.130	0.500	9.000	0.000	99.000
6	113.570	166.960	0.880	872.350	0.000	239.000
7	314.570	637.610	1.340	821.730	0.000	379.000
8	648.000	921.550	13.750	744.440	0.000	519.000
9	2796.260	1538.650	19.020	610.130	53.520	679.000
10	4049.340	2001.620	45.760	335.620	166.000	839.000
11	4700.820	2016.390	44.680	227.240	296.100	1064.500
12	4852.210	1882.500	44.540	141.810	671.640	1602.950
13	4769.000	1661.440	1136.800	100.060	825.200	1873.500
14	4629.000	1535.080	1145.480	60.630	1086.000	1967.980
15	4474.000	1671.510	1176.900	44.690	1289.000	1903.490
16	4281.150	1382.700	1020.930	31.560	1262.000	1562.950
17	4208.220	1019.890	1355.060	17.070	1234.060	906.650
18	3993.600	848.620	1210.160	11.040	1184.650	576.240
19	3857.720	540.460	996.170	6.530	1134.780	144.090
20	3379.000	304.000	761.390	0.000	1086.170	82.900
21	2779.390	0.000	538.900		920.630	34.060
22	1890.160	0.000	139.680		362.270	16.000
23	938.000		66.340		200.640	12.000
24	584.650		33.570		146.000	8.000
25	426.550		25.570		35.630	14.000
26	296.680		14.830		29.000	8.000
27	269.800		10.290		30.040	20.000
28	245.300		8.660		26.480	23.630
29	195.350		5.410		23.070	25.000
30	150.660		4.410		20.810	20.000
31	110.940		4.610		17.000	23.000
32	76.000		2.860		7.000	15.000
33	61.770		1.180		5.340	14.000
34	55.000		1.890		3.140	17.000
35	32.260		0.610		0.000	14.530
36	12.580		0.000			17.120
37	0.000		0.000			16.910
38			0.000			10.970
39						0.000

Table 6 Curve numbers for different landuse and soil type for AMC II

Sl.No.	Landuse	Curve numbers	
		Soil type B	Soil type C
1	Agricultural land	81	88
2	Dense forest	76	82
3	Degraded forest	85	90
4	Eroded land	86	91
5	Reservoir	100	100

Table 7 Adjusted initial abstraction parameter for the different storm events considered for the simulation

Sl.No.	Storm event	Initial abstraction parameter K
1	Event no. 1 (19.8.1983)	1.40
2	Event no. 2 (9.8.1984)	0.36
3	Event no. 3 (30.7.1985)	2.05
4	Event no. 4 (13.8.1985)	0.38
5	Event no. 5 (14.8.1986)	1.67
6	Event no. 3 (26.8.1987)	0.09

Table 8 Rainfall excess using SCS CN method for the storm events considered for the simulation

Time in hours	Event 1 19.8.1983 16 th hour (mm)	Event 2 9.8.1984 21 st hour (mm)	Event 3 30.7.1985 16 th hour (mm)	Event 4 13.8.1985 17 th hour (mm)	Event 5 14.8.1986 17 th hour (mm)	Event 6 26.8.1987 21 st hour (mm)
1	0.000	0.020	0.040	0.001	0.026	0.022
2	0.041	0.032	0.420	1.406	0.141	0.189
3	0.096	0.216	0.375	10.448	0.369	0.502
4	1.943	0.760	0.058	4.120	0.420	1.524
5	10.214	1.352	0.254	0.915	0.126	1.499
6	16.999	3.097	0.655		0.061	1.870
7	4.114	6.784	0.712		0.377	4.748
8	11.949	6.434	0.537		1.368	11.185
9	14.455	11.916	2.433		3.494	2.846
10	16.799	7.530	7.611		3.507	4.005
11	17.262	8.088	8.257		12.463	7.769
12	28.056	13.249	5.482		17.968	13.672
13	29.825	6.169	5.837		7.734	7.513
14	24.571	3.833	2.618		0.000	4.266
15	44.901	0.651	1.271		0.280	
16	8.270	0.124	3.216		0.187	
17	6.386	1.320	1.492		0.026	
18	2.717	2.058			0.429	
19	5.237	2.222			1.455	
20	2.679	0.337			0.053	
21	0.326					

Table 9 Manning's n for different landuses

Sl.no.	Landuse	Manning's n
1	Agricultural land	0.04
2	Dense forest	0.07
3	Degraded forest	0.05
4	Eroded land	0.03
5	Reservoir	0.01

Table 10 Incremental isochronal area for 1 hour interval of time of concentration

Sl.no.	Time of concentration in hour	Incremental isochronal area in sq.km	Cumulative isochronal area in sq.km
1	1	35.313	35.313
2	2	105.688	141.000
3	3	102.188	243.188
4	4	133.625	376.813
5	5	121.688	498.500
6	6	132.688	631.188
7	7	166.938	798.125
8	8	59.000	857.125
9	9	6.000	863.125

Table 11 The simulated direct runoff values for the events considered

Time in hours	Event 1 19.8.1983 16 th hour (cumecs)	Event 2 9.8.1984 21 st hour (cumecs)	Event 3 30.7.1985 16 th hour (cumecs)	Event 4 13.8.1985 17 th hour (cumecs)	Event 5 14.8.1986 17 th hour (cumecs)	Event 6 26.8.1987 21 st hour (cumecs)
1	0.000	0.000	0.000	0.000	0.000	0.000
2	0.000	0.196	0.392	0.010	0.255	0.216
3	0.402	0.901	5.294	13.821	2.146	2.500
4	2.145	3.626	17.144	143.790	8.497	11.097
5	23.041	15.447	24.985	387.089	19.920	35.868
6	161.478	43.569	31.780	478.721	30.153	81.453
7	526.705	101.479	45.119	579.182	35.640	131.442
8	906.210	233.460	65.587	583.931	43.531	225.545
9	1170.750	435.829	90.104	623.531	65.657	436.966
10	1662.324	697.546	119.149	690.315	126.561	693.683
11	2123.766	1051.427	228.092	396.007	222.030	813.921
12	2787.424	1296.068	454.366	109.952	402.881	1013.638
13	3306.561	1656.741	681.459	14.996	836.401	1245.868
14	3628.136	1963.820	880.862	0.000	1274.309	1603.530
15	4275.858	1998.256	1042.646	0.000	1516.623	1775.619
16	5118.555	1994.739	1139.742	0.000	1624.194	1571.484
17	5804.297	1648.527	1242.275	0.000	1583.726	1380.810
18	5609.997	1372.654	1149.284	0.000	1572.780	1342.116
19	5629.249	1190.491	875.430	0.000	1343.188	1182.428
20	4885.584	790.768	661.693	0.000	697.123	729.693
21	4056.865	482.982	427.996		199.770	320.951
22	3336.843	291.550	270.811		79.536	69.915
23	1726.586		224.953		84.231	0.000
24	817.521		121.893		71.232	0.000
25	526.331		24.452		75.739	0.000
26	397.137		0.000		76.455	0.000
27	222.074		0.000		26.304	0.000
28	59.023		0.000		0.869	0.000
29	5.343		0.000		0.000	0.000
30	0.000		0.000		0.000	0.000
31	0.000		0.000		0.000	0.000
32	0.000		0.000		0.000	0.000
33	0.000		0.000		0.000	0.000
34	0.000		0.000		0.000	0.000
35	0.000		0.000		0.000	0.000
36	0.000		0.000		0.000	0.000
37	0.000		0.000		0.000	0.000
38			0.000			0.000
39						0.000

**Table 12 Peak flow and time to peak flow of observed and simulated direct runoff
for the events considered**

Event no.	Peak flow (cumecs)			Time to peak (Hour)		
	Observed	Simulated	% Error	Observed	Simulated	% Error
1	4852.210	5804.297	19.52	11	16	45.45
2	2016.390	1998.256	0.89	10	14	40.00
3	1355.060	1242.275	8.32	16	16	0.00
4	872.350	690.315	20.86	5	9	80.00
5	1289.000	1624.194	26.00	14	15	7.14
6	1967.980	1775.619	9.77	13	14	7.69

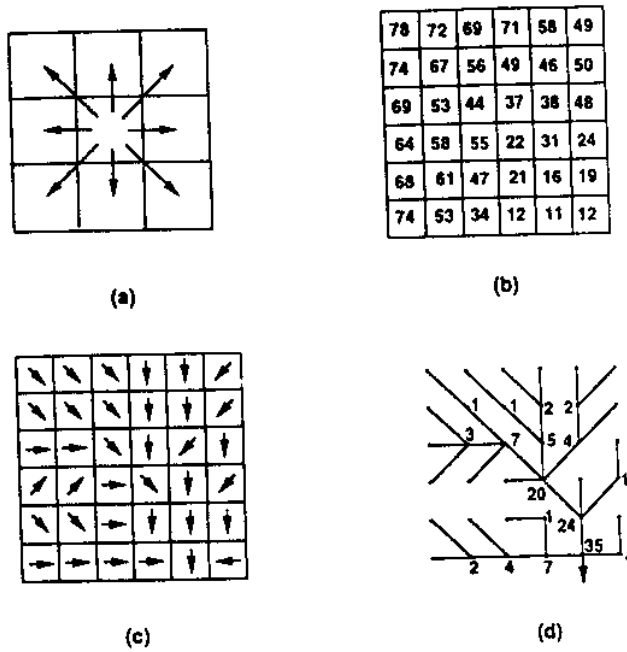


Figure 1 Watershed terrain analysis using grid GIS methods: (a) the eight-direction pour point model; (b) a grid of terrain elevations; (c) the corresponding grid of flow directions; (d) the equivalent network showing flow accumulation

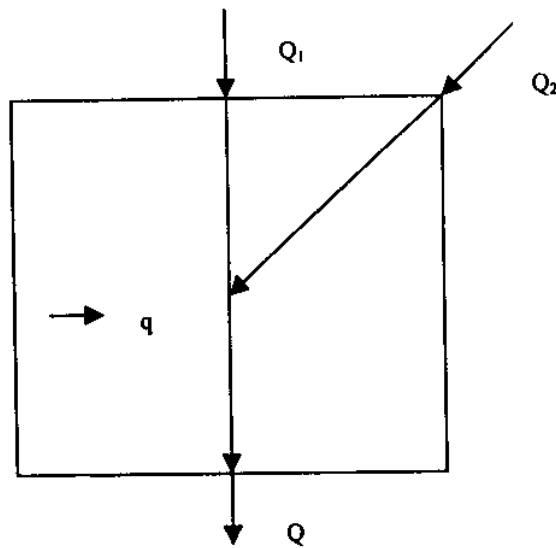
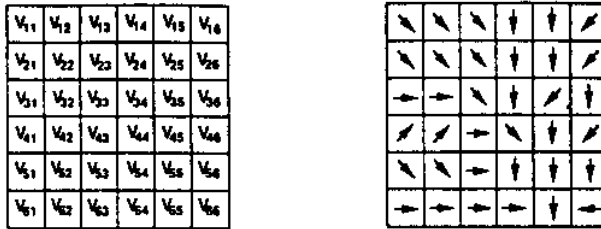
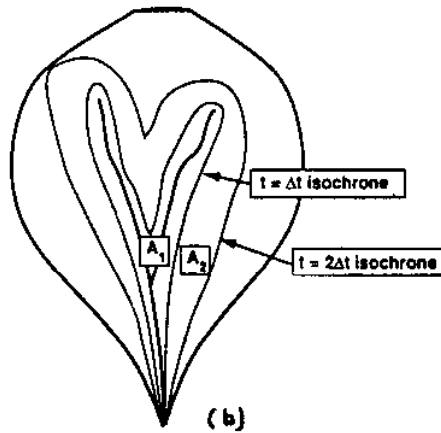


Figure 2 Flow routing in the cell



(a)



(b)

Figure 3 Watershed time-area relationships: (a) a velocity field specified by the magnitude and direction of flow velocity; (b) a watershed isochrone map drawn by classifying a grid of time of flow to the outlet

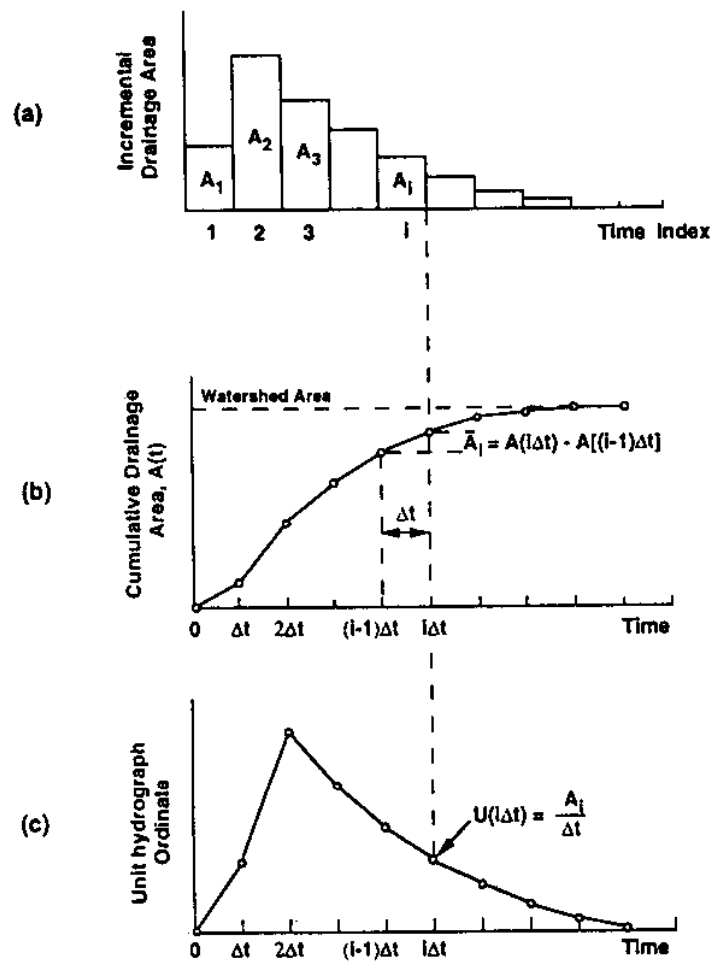


**Figure 4 The time-area diagram and the unit hydrograph:
 (a) incremental drainage area; (b) the cumulative time-area diagram;
 (c) unit hydrograph found as the slope of the time-area diagram**

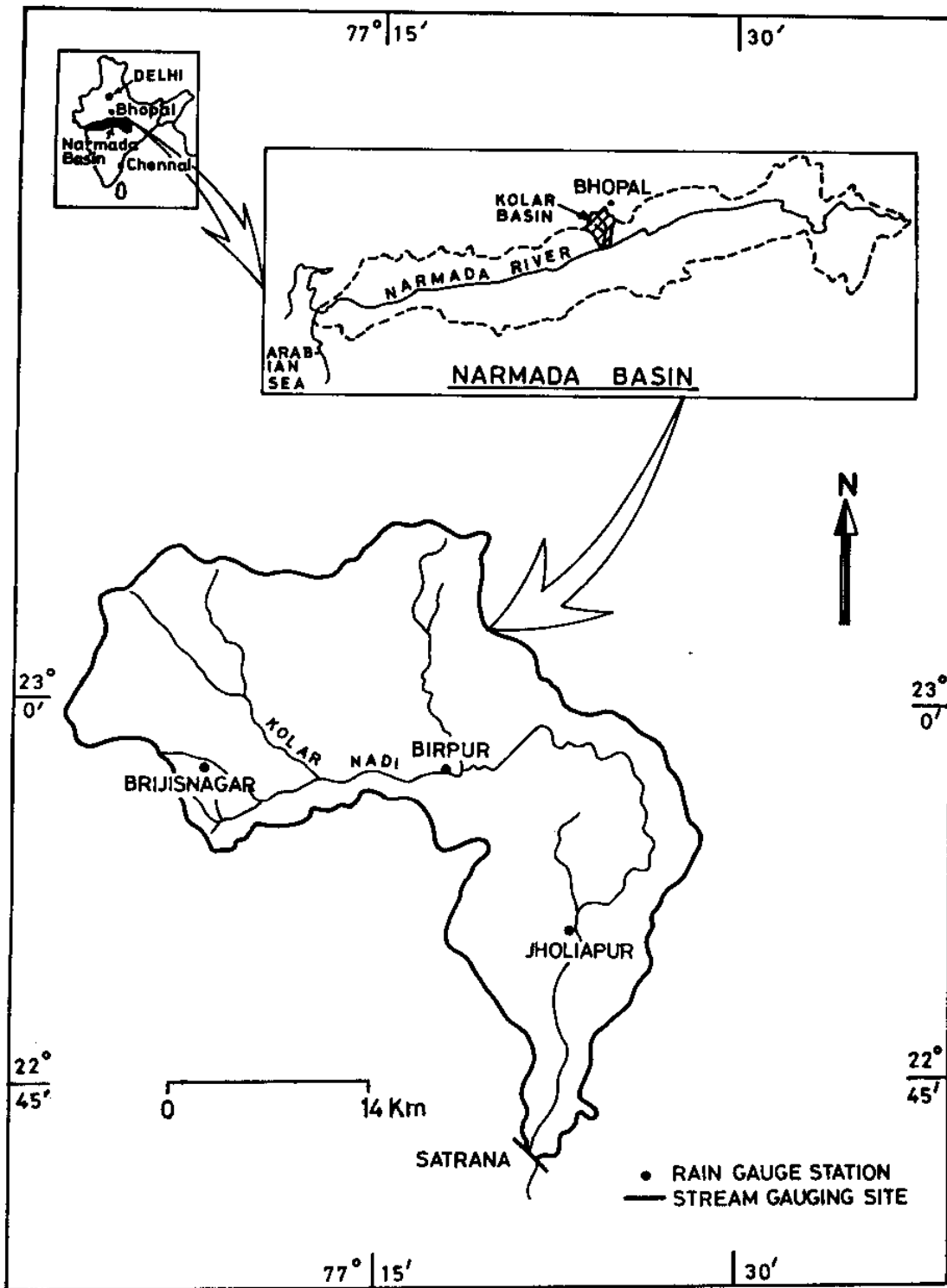


FIG. 5 INDEX MAP OF KOLAR BASIN UPTO SATRANA GAUGING SITE

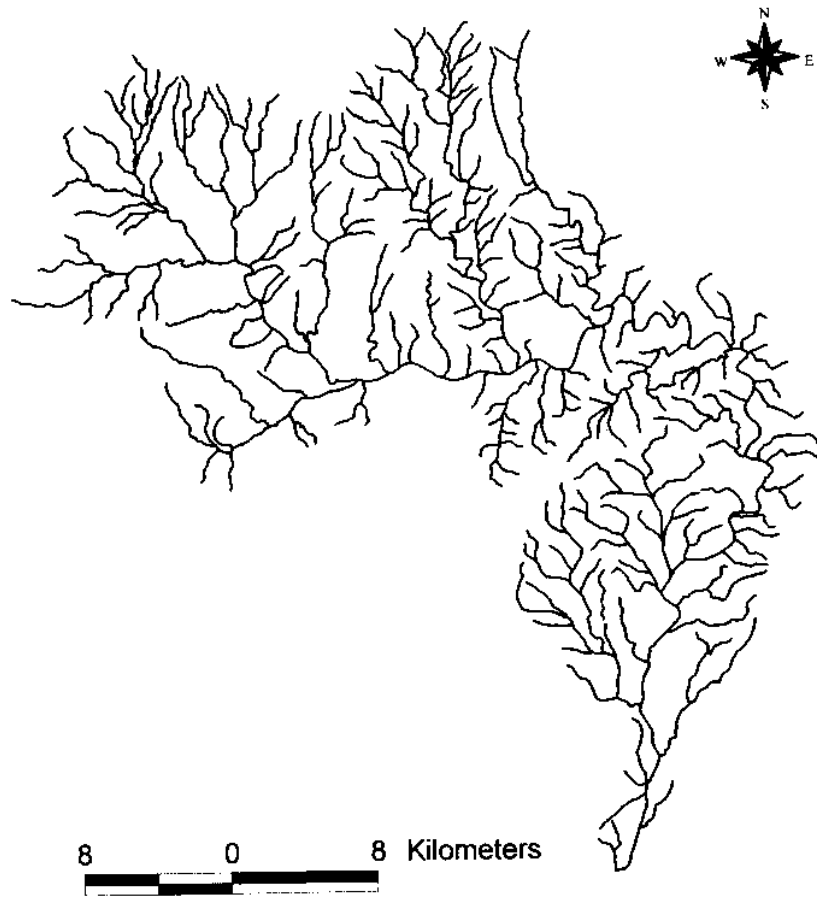
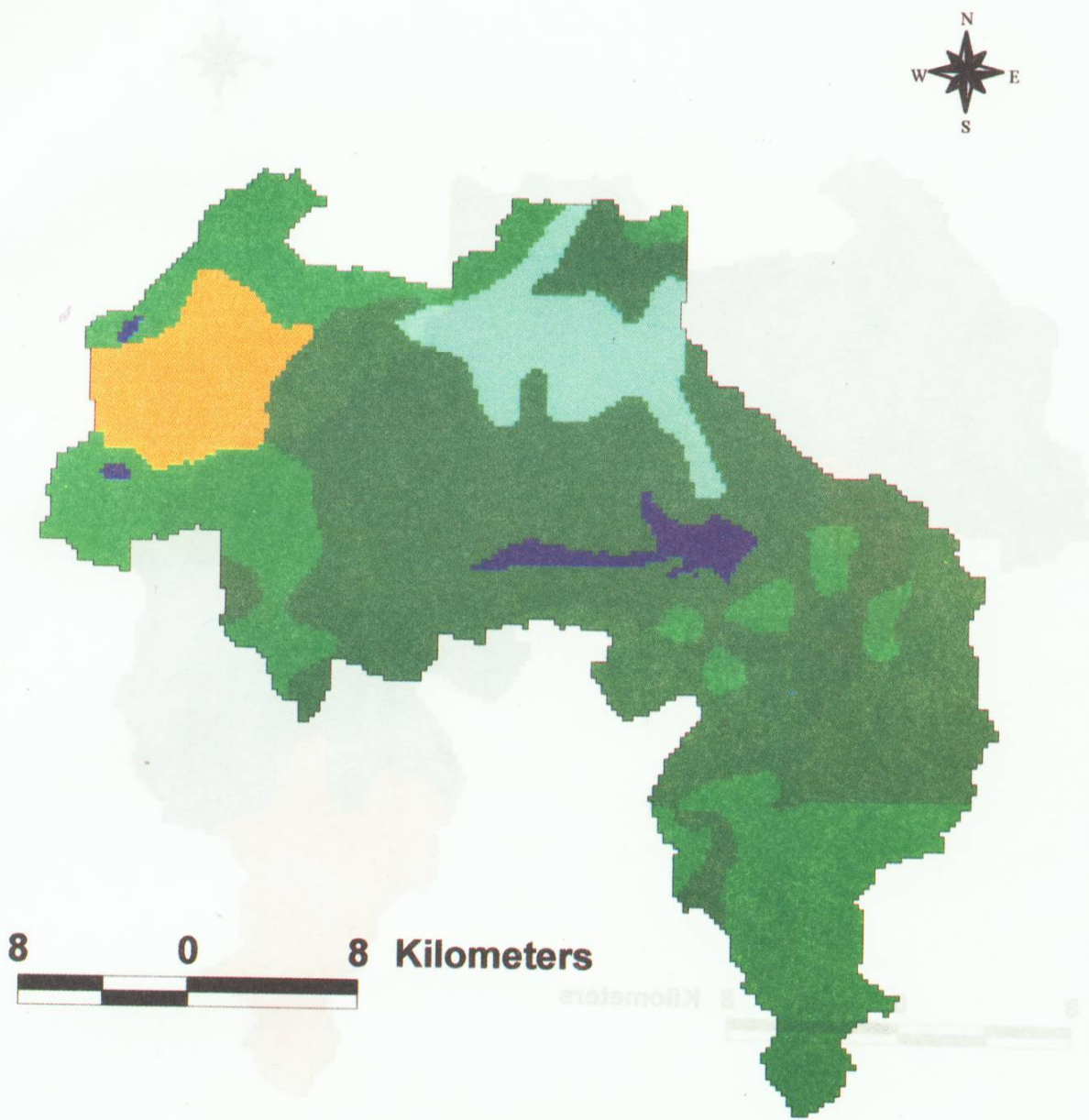
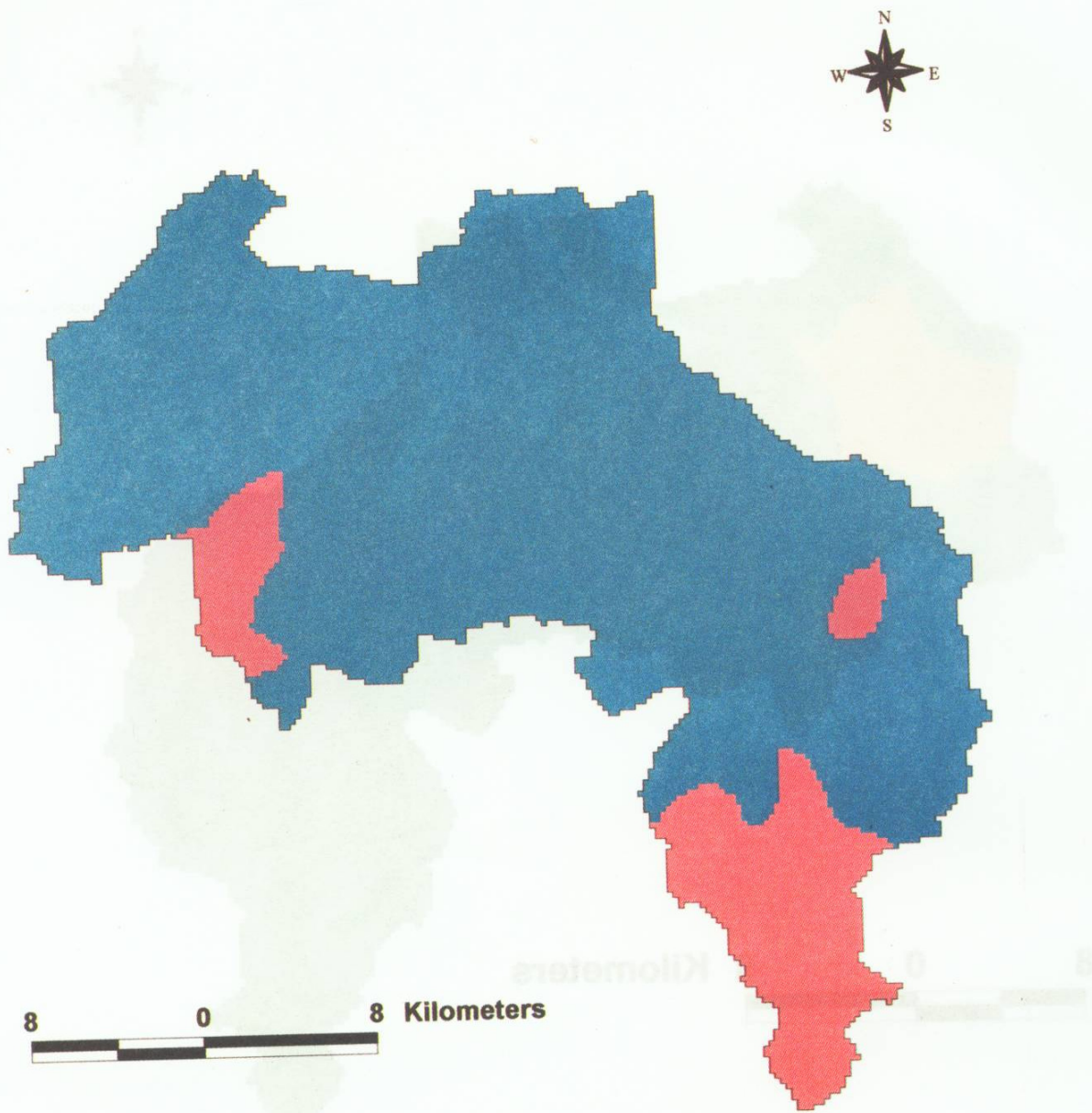


Figure 6 Drainage Map for Kolar Basin



- Landuse**
- Agricultural land
 - Dense forest
 - Degraded forest
 - Eroded land
 - Reservoir

Figure 7 Land use map for Kolar basin



Soil Group
 Group B
 Group C

Figure 8 Soil group map for Kolar basin

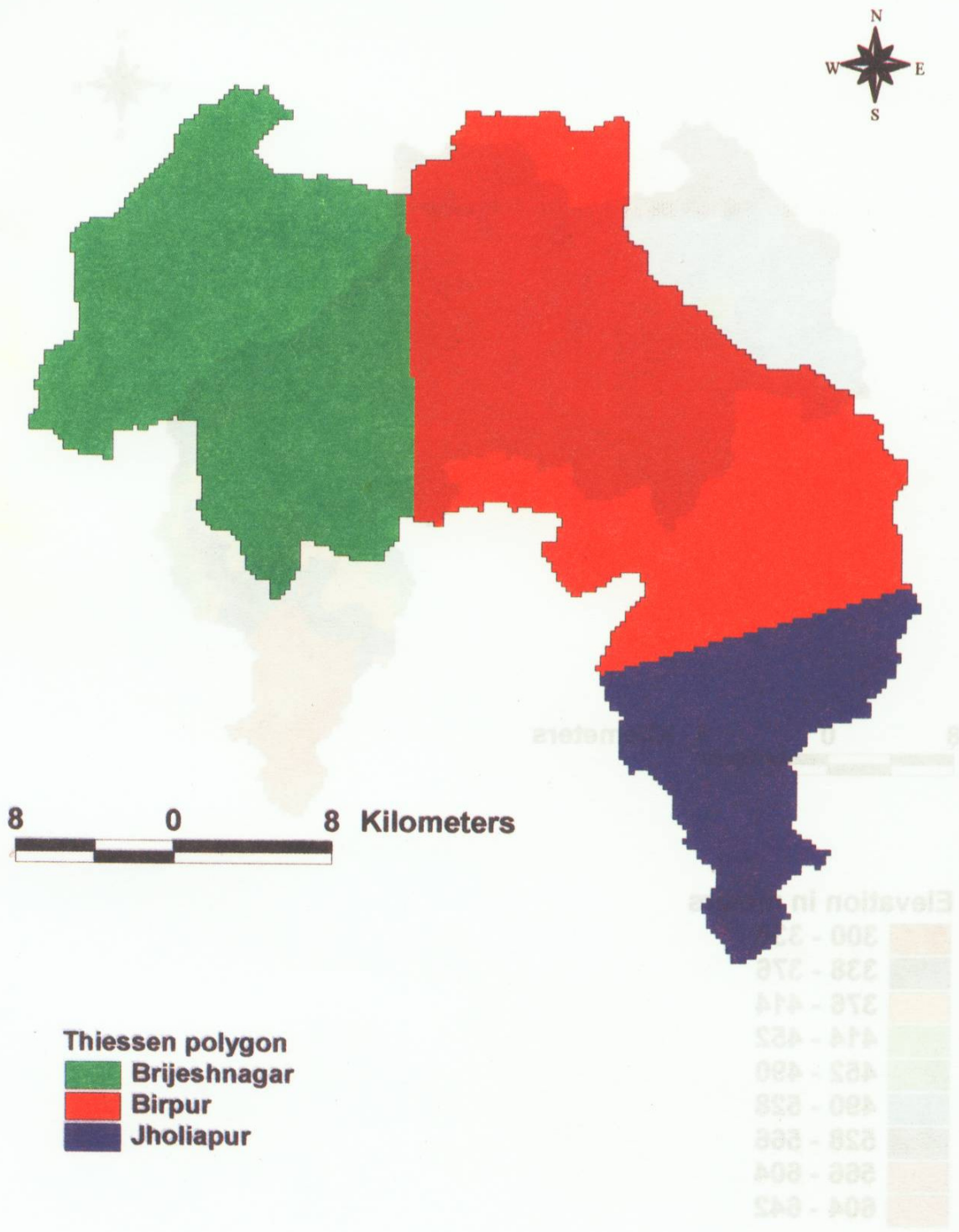


Figure 9 Thiessen polygon map for Kolar basin

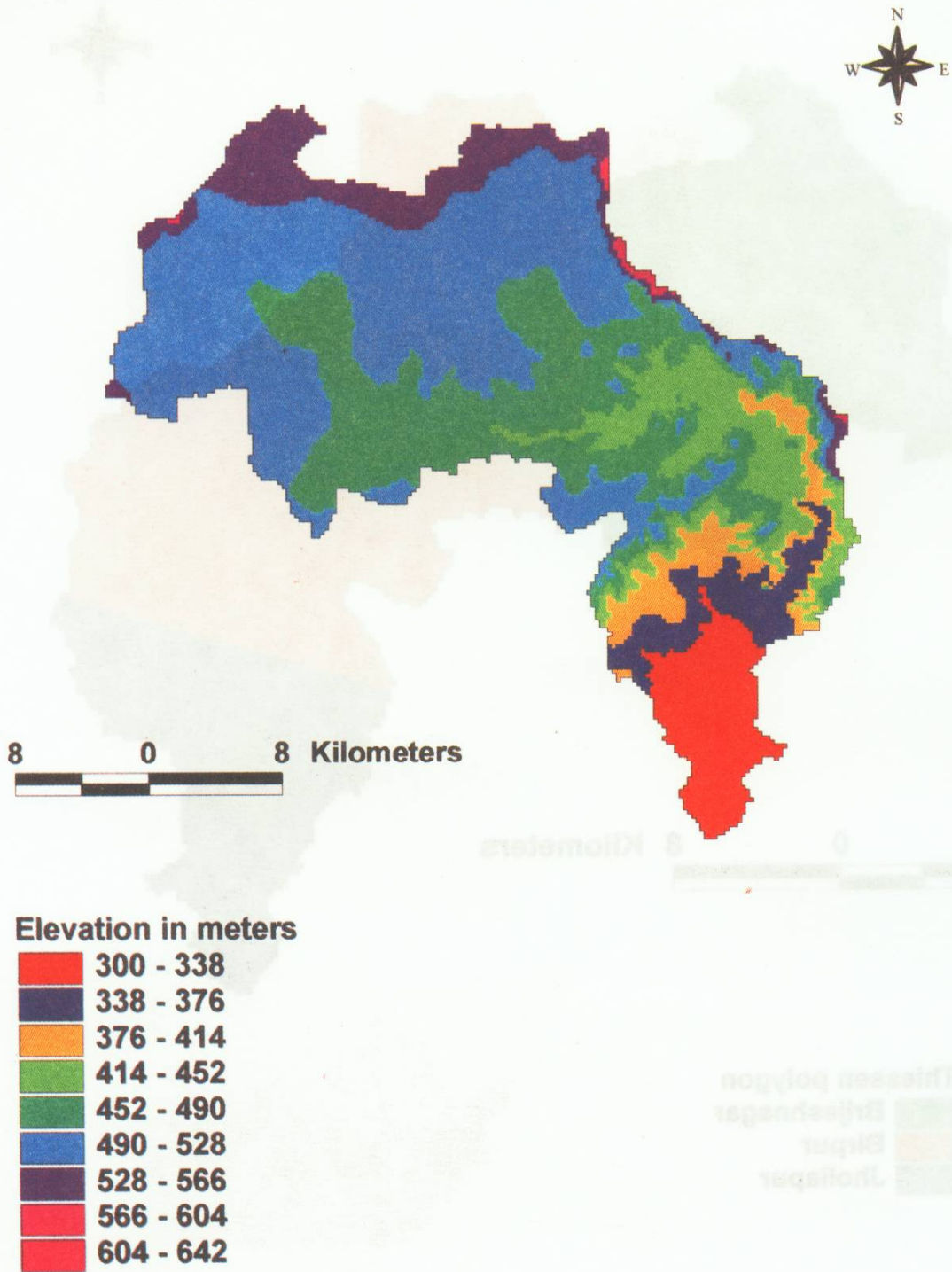


Figure 10 Digital Elevation Model (DEM) for Kolar basin

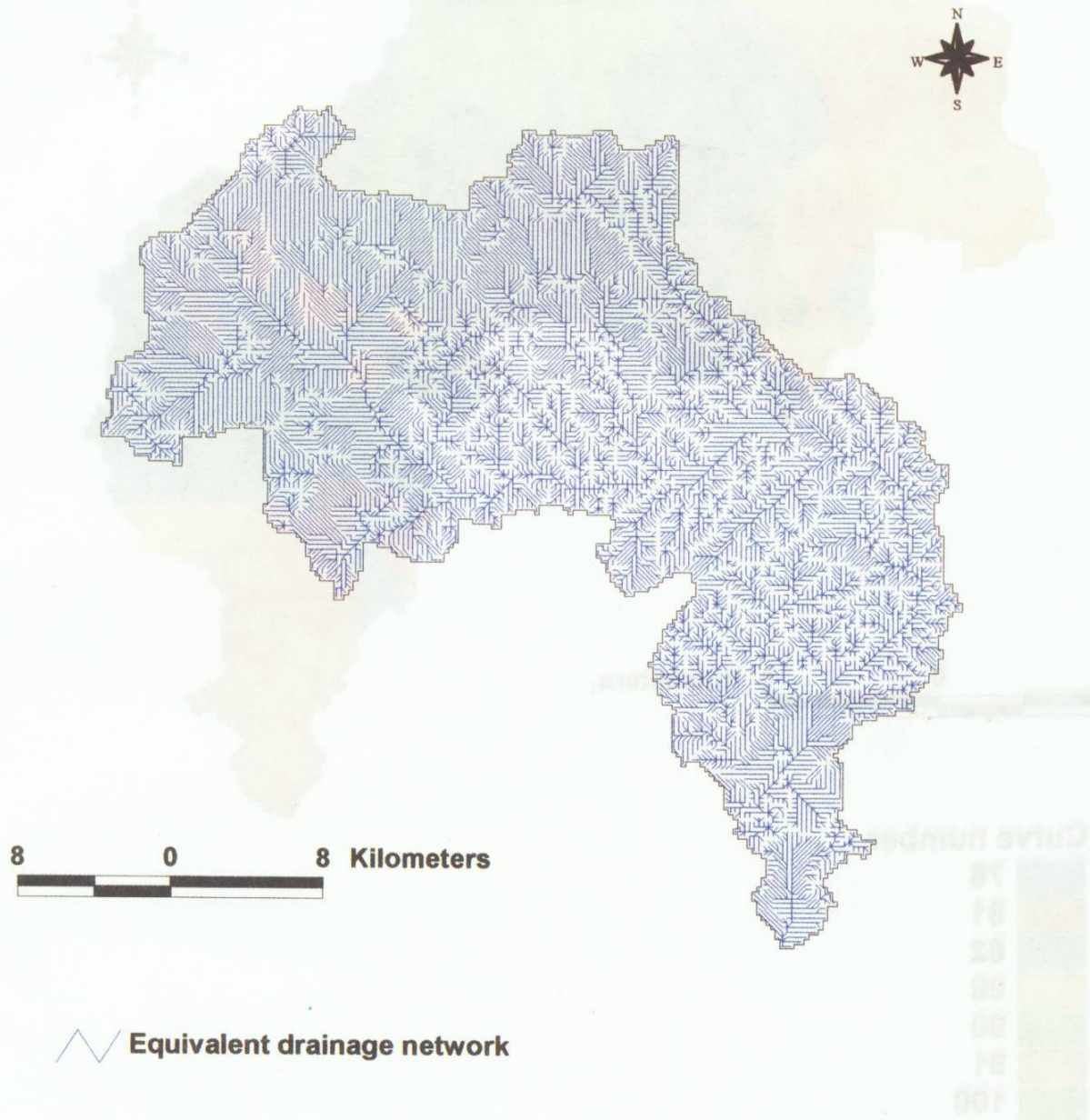


Figure 11 Equivalent drainage network for Kolar basin

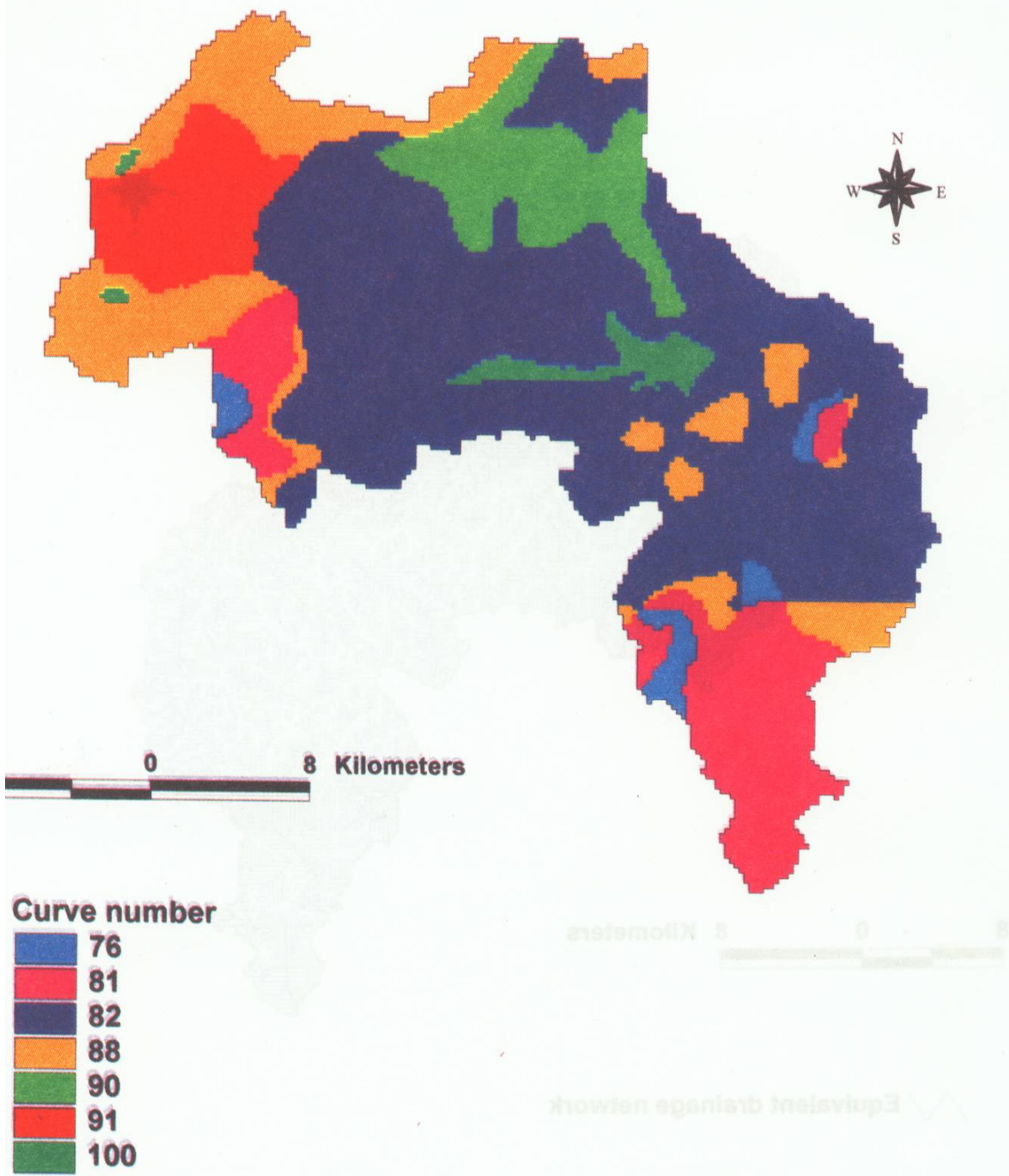


Figure 12 Curve number map for Kolar Basin

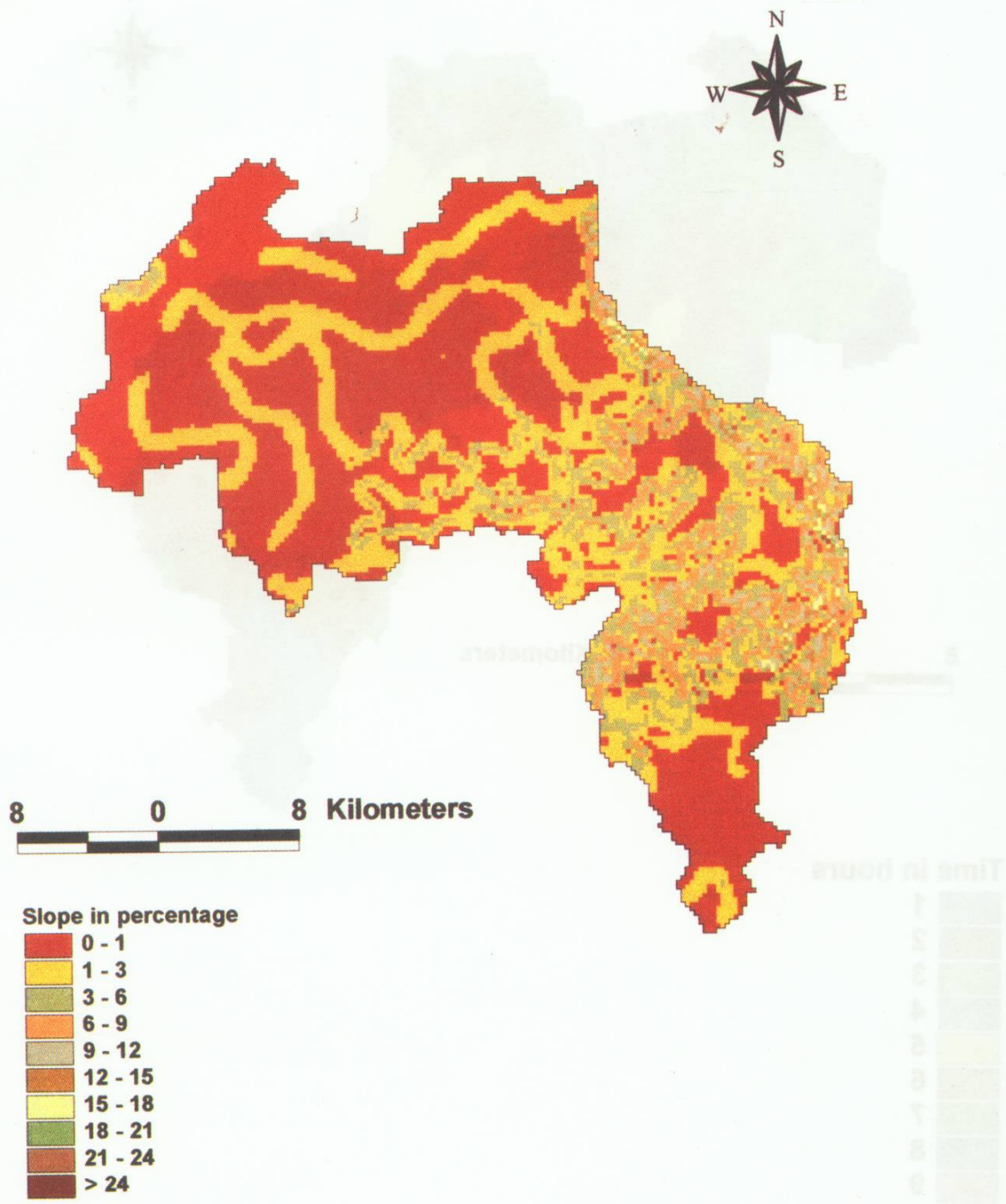


Figure 13 Slope map for Kolar basin

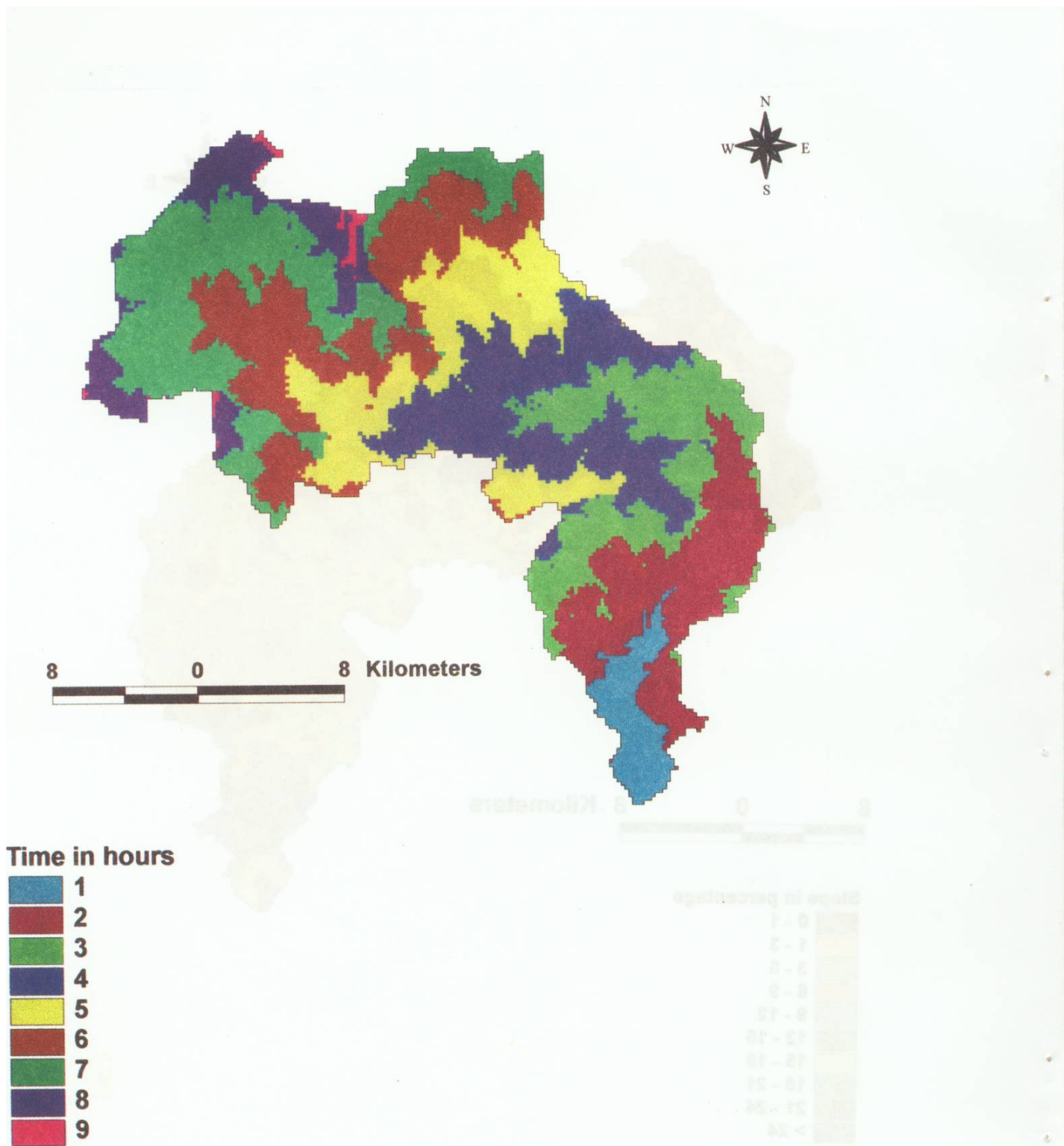


Figure 14 Isochrone map for Kolar basin

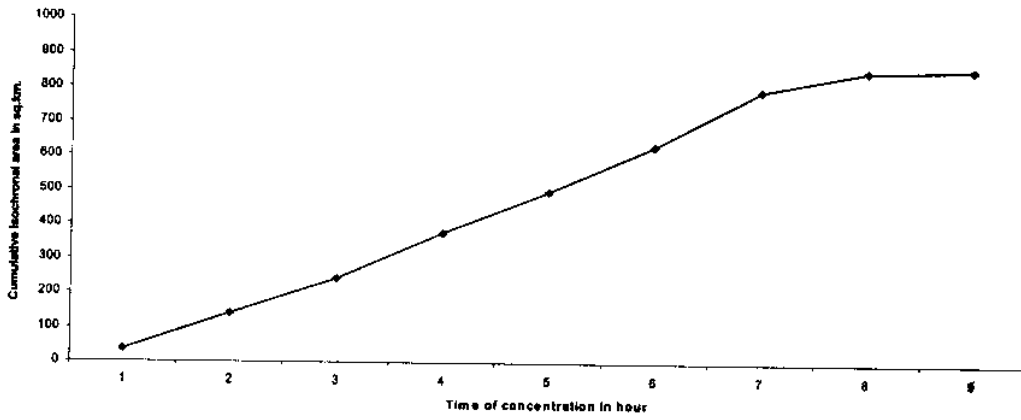


Figure 15 Time-area diagram for Kolar basin

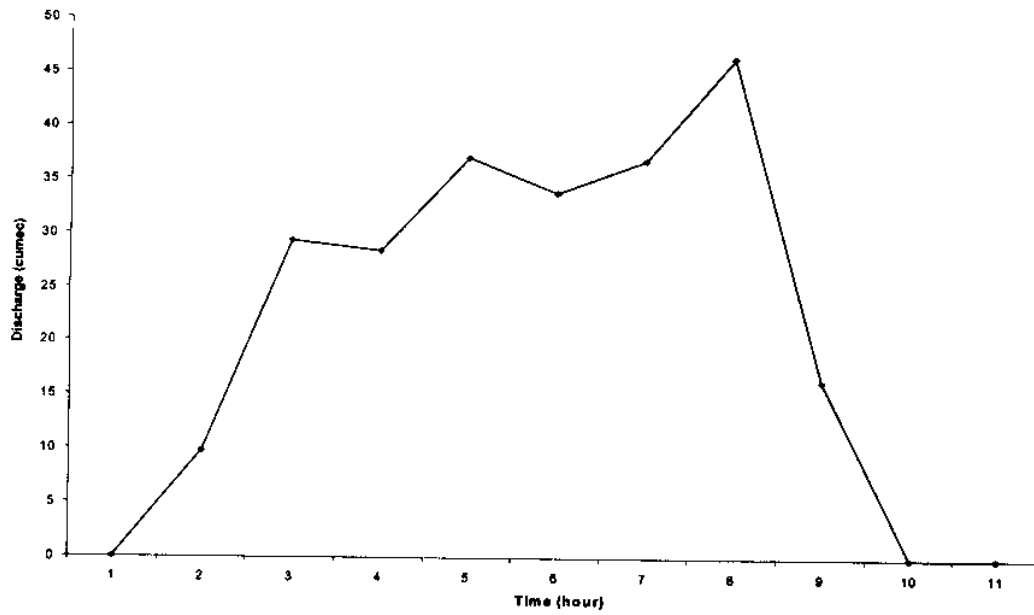


Figure 16 One hour distributed unit hydrograph

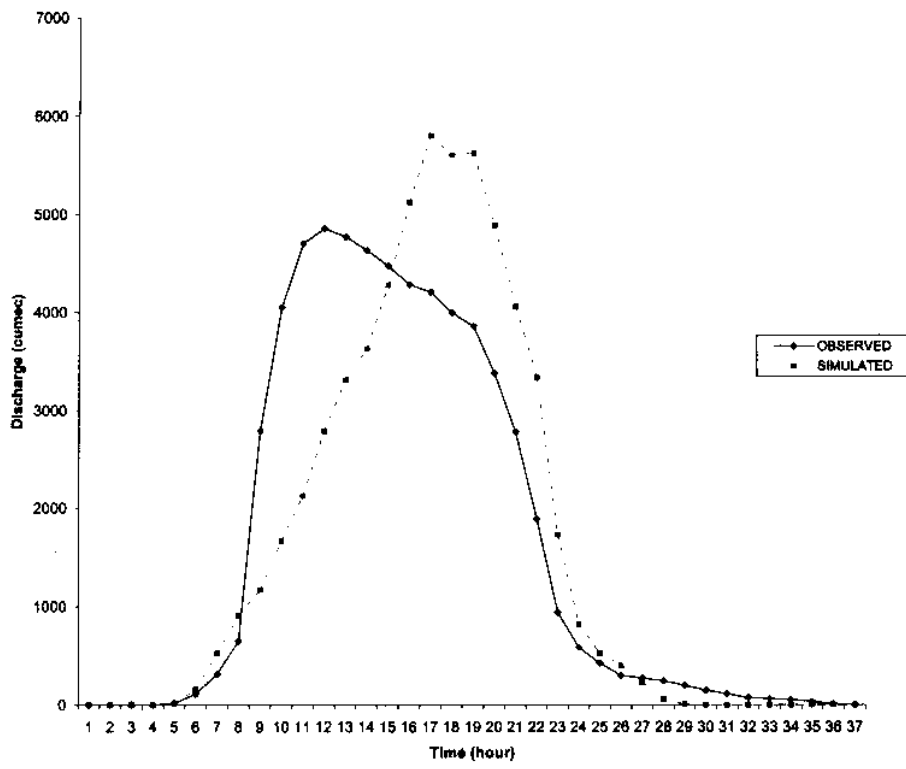


Figure 17 Observed and simulated runoff for the storm event 1 (19.8.1983)

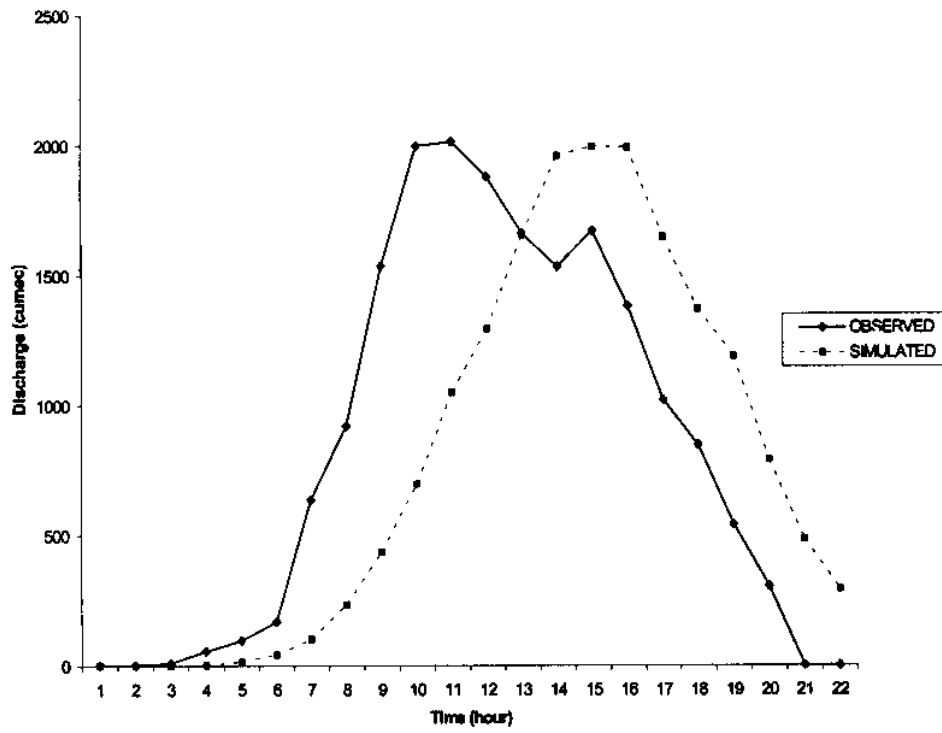


Figure 18 Observed and simulated runoff for the storm event no. 2 (9.8.1984)

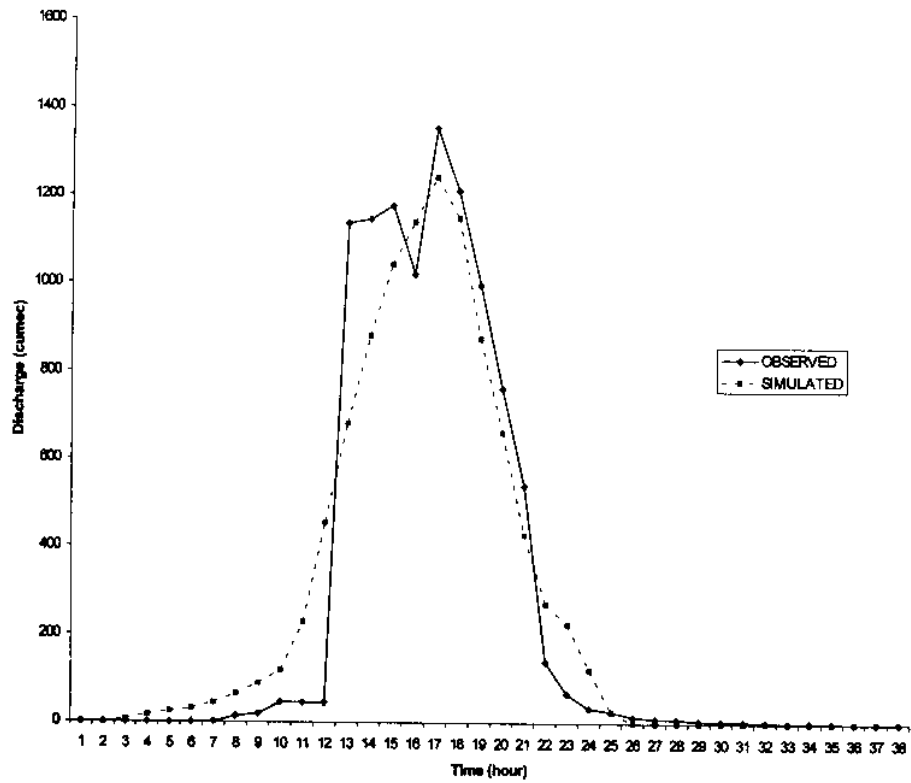


Figure 19 Observed and simulated runoff for the storm event no. 3 (30.7.1985)

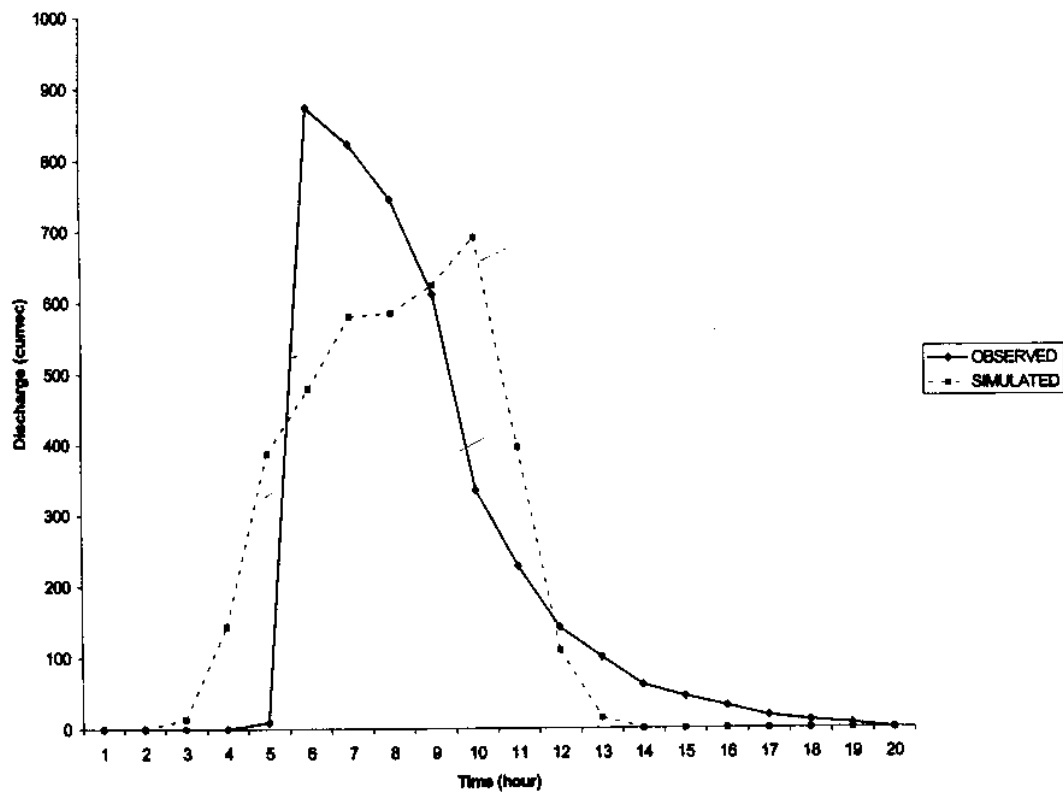


Figure 20 Observed and simulated runoff for the storm event no. 4 (13.8.1985)

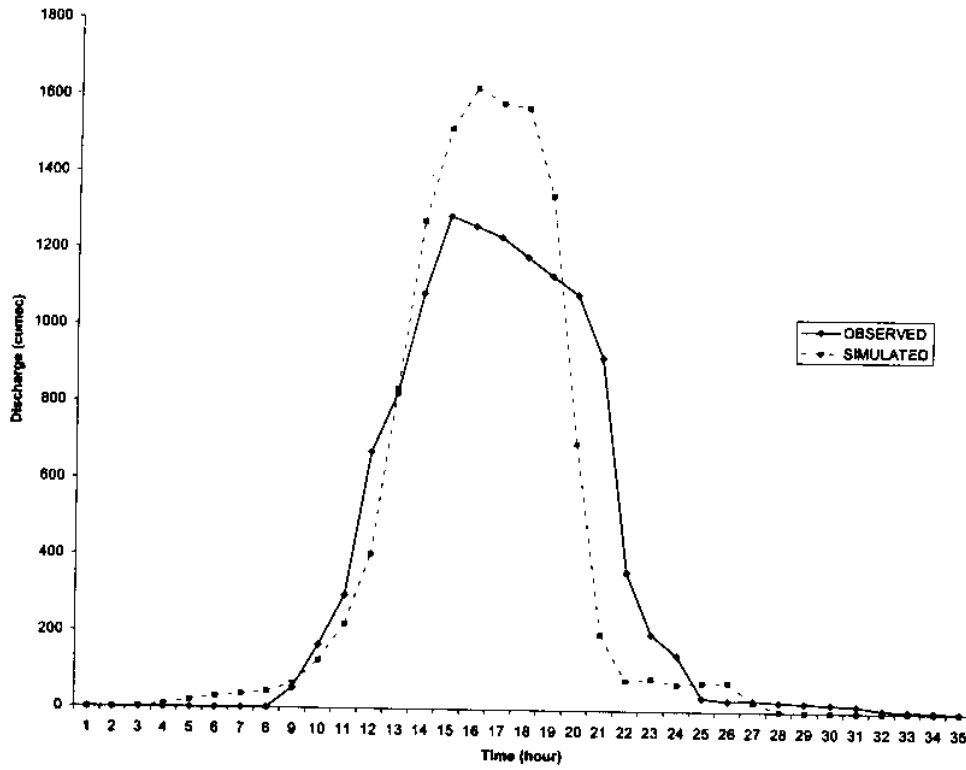


Figure 21 Observed and simulated runoff for the storm event no. 5 (14.8.1986)

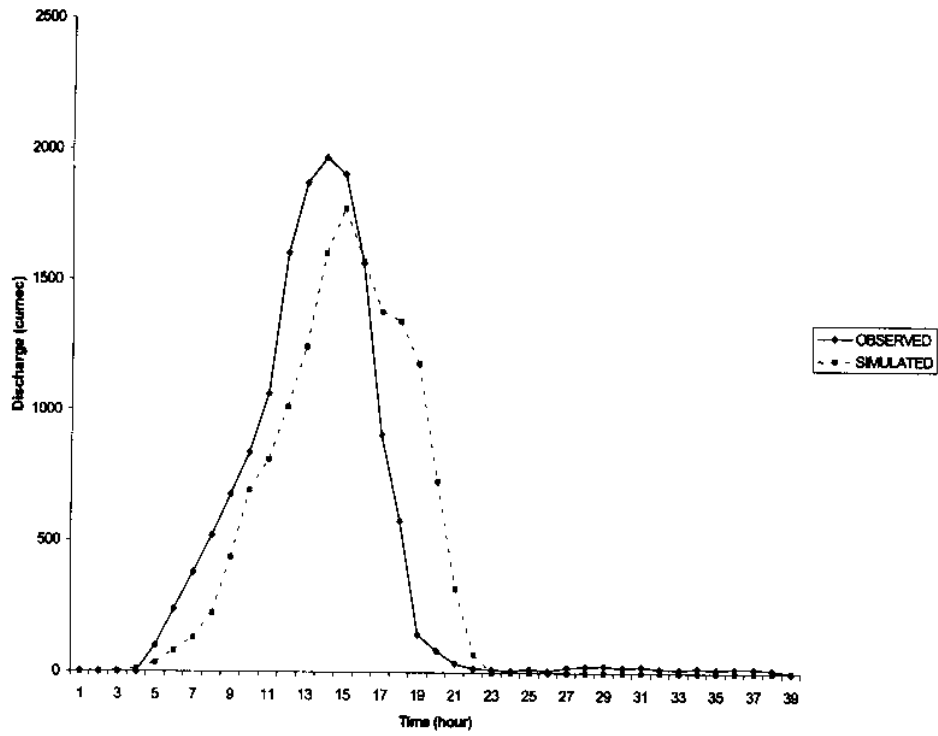


Figure 22 Observed and simulated runoff for the storm event no. 6 (26.8.1987)

STUDY GROUP

Director : Dr K S Ramasastrri

Head : Dr S K Jain

Scientist : Sh A R Senthil kumar
Sh M K Jain

Scientific Staff : Sh P K Agarwal